NATIONAL ADVISORY COMMITTEE FOR AERONAUTICS

TECHNICAL NOTE 4339

HYDRODYNAMIC IMPACT LOADS OF A -20° DEAD-RISE INVERTED-V MODEL AND COMPARISONS WITH LOADS OF A FLAT-BOTTOM MODEL

By Philip M. Edge, Jr.

Langley Aeronautical Laboratory
Langley Field, Va.

Washington
August 1958

NATIONAL ADVISORY COMMITTEE FOR AERONAUTI(

TECHNICAL NOTE 4339

HYDRODYNAMIC IMPACT LOADS OF A -20° DEAD-RISE INVERTED-V MODEL AND COMPARISONS WITH LOADS OF A FLAT-BOTTOM MODEL

By Philip M. Edge, Jr.

SUMMARY

As part of a study of hydrodynamic impact loads on chine-immersed bodies, a model having an inverted-V transverse shape and a dead-rise angle of -20° was tested at the Langley impact basin. A series of fixed-trim impacts of this inverted-V model were made in smooth water over a wide range of trim and initial flight-path angles at a beam-loading coefficient of 19.15 with a few impacts at beam-loading coefficients of 27.90 and 36.07.

The data are presented in tables and in figures as variations of loads and motions (in coefficient form) with time, trim angle, and flight-path angle. In general, the maximum impact loads experienced by the inverted-V model were greater than the loads which have been obtained for a flat-bottom model; however, for the severe impact conditions approaching 0° trim (flat impacts) a trend toward smaller loads than those experienced on a flat bottom is indicated. Peak pressures for the inverted-V transverse shape compare with those for the flat-bottom model in a manner similar to the maximum impact loads.

INTRODUCTION

Investigations of hydrodynamic impact loads on chine-immersed bodies at the Langley impact basin have included several transverse shapes (refs. 1 to 4). Reference 1 presented loads for a flat-bottom (0° dead-rise angle) model and references 2 to 4 presented loads for models having positive dead-rise angles and V and curved transverse shapes. These investigations have indicated the relation of maximum loads to transverse shape for chine-immersed models of zero and positive dead-rise angles. The present investigation extends this study beyond the flat plate to the inverted-V shape with a -20° dead-rise angle.

Configurations having negative dead-rise angles are of interest from the standpoint of the unconventional flow of water from the instant of initial contact as compared with impacts of bodies having positive

dead-rise angles. The flow upon initial contact of the model having a negative dead-rise angle is from the chines inward toward the center or keel of the bottom as contrasted with that of the model having a positive dead-rise angle which is outward from the keel. This difference in flow is closely related to the spray and loads produced during impact. Whereas on bottoms having positive dead-rise angles chine strips or chine curvatures are required to divert the flow of water from airplane structures, engine inlets, and so forth, the transverse shape with a negative dead-rise angle is expected to confine the spray toward the center of the hull or hydro-ski. The gradual immersion of the cross section with a negative dead-rise angle is similar to that of the cross section with a positive dead-rise angle and, therefore, some similarity can be expected in the application of the impact load. However, the inward flow during the impact of a model with a negative dead-rise angle tends to pile up water at the keel and thereby affects the load quite differently than does the outward flow of bodies having positive dead-rise angles.

The purpose of this investigation was to determine the effect of a negative dead-rise angle on the hydrodynamic impact loads over a range of landing conditions. A prismatic model with this type of transverse shape and a straight keel was subjected to a series of fixed-trim impacts in smooth water at the Langley impact basin. Most of the impacts were made at a beam-loading coefficient of 19.15 and covered a range of trim and initial flight-path angles; however, a few impacts were made at beam-loading coefficients of 27.90 and 36.07. The total loads and pitching moments together with the motions of the fixed-trim model were measured during the impact process. Also, impact pressures were measured at several points along the model.

This report contains tables of the basic data from the investigation and presents variations of the loads and motions with time, with initial flight-path angle, and with trim angle. The maximum loads and maximum measured pressures obtained for the inverted-V model are compared with those previously obtained for a flat-bottom model.

SYMBOLS

b	model beam, ft
$\dot{f}$	equivalent planing velocity, $\frac{V_n}{\sin \tau}$, ft/sec
F_n	hydrodynamic force normal to keel, lb

F_V	vertical component of hydrodynamic force, lb
g	acceleration due to gravity, 32.2 ft/sec^2
l	wetted length of model at chine, ft
M_Y	pitching moment about step, lb-ft
n_i	impact load factor normal to undisturbed water surface, $\frac{F_V}{W}$
p	pressure, lb/sq in.
t	time after water contact, sec
V	resultant velocity of model, ft/sec
V_n	velocity of model normal to keel, $\dot{x} \sin \tau + \dot{z} \cos \tau$, ft/sec
W	dropping weight, lb
$\dot{x}$	velocity of model parallel to undisturbed water surface, ft/sec
z	draft of model normal to undisturbed water surface, ft
$\dot{z}$	velocity of model normal to undisturbed water surface, ft/sec
γ	flight-path angle relative to undisturbed water surface, deg
ρ	mass density of water, 1.938 slugs/cu ft
τ	trim angle, deg
C_{cp}	center-of-pressure coefficient, $\frac{\text{Center of pressure measured from step}}{b}$
C_d	draft coefficient, $\frac{z}{b}$
C_L	impact lift coefficient, $\frac{n_i W}{\frac{1}{2}\rho V_o^2 b^2}$

C_m pitching-moment coefficient, $\frac{M_Y}{\frac{1}{2}\rho V_o^2 b^3}$

C_t time coefficient, $\frac{V_o t}{b}$

$C_{\dot{z}}$ vertical-velocity coefficient, $\frac{\dot{z}}{\dot{z}_o}$

C_Δ beam-loading coefficient, $\frac{W}{\rho g b^3}$

Subscripts:

o instant of contact with water surface

max maximum

APPARATUS

Tests were made in the Langley impact basin with the equipment described in reference 5. This equipment consists of a catapult, an arresting gear, associated instrumentation for measuring loads and motions of the model, and a testing carriage to which the model is attached at all times by a boom. The boom is mounted on a parallel linkage which permits the model to move freely in the vertical direction while the carriage is moving horizontally down the tank.

Model

A cross section of the inverted-V model is shown in figure 1 and the installation of the model on the carriage boom is shown in figure 2. The inverted-V model had a -20° angle of dead rise, a 1-foot beam, and a straight keel and chine 12 feet long. The bottom was of wood covered with fiber glass and the remainder of the model, which included a 2-foot nose section forward of the bottom, was of sheet-metal construction.

Instrumentation

The instrumentation consisted of a multichannel oscillograph, accelerometers, a dynamometer, water-contact indicator, and electrical

circuits for measuring displacements, velocities, and pressures. All measurements were recorded on the oscillograph together with 0.01-second timing.

Accelerations in the vertical direction were measured by strain-gage-type accelerometers having undamped natural frequencies of 17 and 120 cycles per second. The load normal to the keel of the model and pitching moments about the step were obtained from a strain-gage-type dynamometer mounted between the model and the carriage boom (fig. 2) and from consideration of the inertia effects of the mass below the dynamometer.

The initial contact of the model with the water and rebound from the water were determined from an oscillograph record of a pulse produced by an electrical circuit which was completed by the water through contacts in the model. Horizontal velocity was computed from photoelectric-cell indications of horizontal displacement and from the time increments. Measurements of vertical displacement were obtained from a slide wire and vertical velocity was obtained from electrical differentiation of the slide-wire displacement.

Impact pressures were obtained from ten pressure gages flush-mounted in the bottom at the locations shown in figure 3. The pressure gages were of the inductive type except for gage 10 which was of the unbonded strain-gage type. All gages had a diaphragm diameter of 1/2 inch. The signals from the pressure gages were amplified and recorded with a flat frequency response extending to above 1,000 cycles per second.

In general, the data obtained in this investigation are believed to be accurate within the following limits:

Horizontal velocity, ft/sec	±0.5
Vertical velocity, ft/sec	±0.2
Vertical displacement, ft	±0.02
Acceleration, g units	±0.2
Pressure, lb/sq in.	±3
Weight, lb	±10
Time, sec	±0.002
Pitching moment, percent	±5

The gradual application of the load under some impact conditions led to uncertainty in determining the instant of peak reading on flat load and moment curves. Consequently, the determined times to peak are not as accurate as the above values indicate.

TEST PROCEDURE

This investigation consisted of a series of fixed-trim impacts in smooth water for landing conditions covering a range of trims and flight-path angles. Impacts were made at trim angles of 0°, 4°, 8°, 12°, 16°, 20°, and 30° and over a range of flight-path angles from 3° to 25° with a few impacts without forward speed ($\gamma_o = 90^\circ$) at $\tau = 0^\circ$ and 8° (velocity range: $\dot{z}_o = 3.9$ to 12.2 feet per second, $\dot{x}_o = 0$ to 80 feet per second). The impacts were made at a beam-loading coefficient of 19.15 ($W = 1{,}195$ pounds). In order to check effects of beam loading, a few impacts were made at beam-loading coefficients of 27.90 and 36.07 ($W = 1{,}741$ and 2,251 pounds, respectively) for 8° trim over a range of flight-path angles ($\dot{z}_o = 4.5$ to 12.4 feet per second, $\dot{x}_o = 31$ to 72 feet per second).

During each impact a lift force equal to the weight of the model and drop linkage was applied to simulate a wing lift of 1 g (ref. 5). Several times during the test, repeat impacts were made to check the consistency of the behavior of the equipment and instruments. No significant changes were observed and the data of these repeat impacts were averaged for presentation in this report.

RESULTS AND DISCUSSION

The experimental data obtained in this investigation are presented in tables I and II for each of the impacts. Table I presents the measured values of loads and motions at contact with water, at maximum acceleration, at maximum pitching moment, at maximum draft, and at rebound. Table II shows the maximum pressures measured at the pressure-gage locations (fig. 3) and the vertical velocity at the time of each maximum pressure for each of the impacts. Some of the measurements were not successfully obtained (noted in the tables by dashes) because the magnitude was out of range of the instrument or because the instrument failed to function.

Time Histories

Variations of the load, draft, vertical velocity, and pitching moment are shown in figures 4 to 7 in coefficient form. The data for impacts without forward speed are shown in figures 4 and 5 for two values of $\dot{z}_o$ at $\tau = 0^\circ$ and 8° and $C_\Delta = 19.15$. From these time histories and from table I it is seen that for a model of the length tested the lift coefficient at 0° trim is significantly greater than the lift

coefficient at 8° trim, maximum lift for impacts at 0° trim being about nine times the lift for impacts at 8° trim. The data for typical impacts with forward speed are shown in figure 6 for $C_\Delta = 19.15$ and in figure 7 for $C_\Delta = 36.07$. These time histories indicate that the loads are largely dependent upon flight-path angle and beam loading and at high flight-path angles are dependent on trim angle. These time histories show that the application of the loads to the inverted-V model is closely similar to the application generally expected for models having positive dead-rise angles.

The inward flow of the water during impact of the inverted-V model might be expected to affect drastically the application of the load so as to create water hammer or shock. However, as shown by the time histories, the loads during the impact were applied smoothly without any detrimental effects from the inward flow.

Variations of Loads and Motions With Trim and Flight-Path Angle

The variations with initial flight-path angle of the coefficients of vertical load, vertical velocity, draft, pitching moment, center of pressure, and time for trim angles of 4°, 8°, and 30° at $C_\Delta = 19.15$ are presented in figures 8 to 13. In these figures the following significant data are shown:

Impact lift at $n_{i,max}$ and at z_{max} (fig. 8)
Draft at $n_{i,max}$ and at z_{max} (fig. 9)
Vertical velocity at $n_{i,max}$ and at exit (fig. 10)
Time at $n_{i,max}$, at z_{max}, and at exit (fig. 11)
Pitching moment at $n_{i,max}$ and at $M_{Y,max}$ (fig. 12)
Center of pressure at $n_{i,max}$ and at $M_{Y,max}$ (fig. 13)

As indicated in table I, during some of the impacts at low trim angles ($\tau = 4°$), the bow of the model became involved before full immersion was reached. In order to eliminate possible effects of the arbitrarily shaped nose of the model, any data obtained after bow immersion were not included.

In general, the data shown in figures 8 to 13 indicate that the loads, moments, and motions of the model having a negative dead-rise angle vary with initial flight-path angle and trim in a manner similar to variations obtained with models having positive dead-rise angles. It is noted that

from figures 12 and 13 comparisons can be made between the pitching-moment and center-of-pressure coefficients at maximum acceleration and the coefficients obtained at maximum pitching moment. This comparison shows that at 30° trim angle the pitching-moment coefficient at $n_{i,max}$ is very close to the maximum. However, as the trim angle is lowered to 8° and 4°, the maximum pitching moment is as much as 25 percent greater than the pitching moment at $n_{i,max}$. Similarly, the center-of-pressure coefficients at $n_{i,max}$ and at maximum pitching moment are about the same at 30° trim, whereas at 4° trim the center of pressure at maximum pitching moment is as much as four times the value at $n_{i,max}$.

Figure 14 presents a summary of the variations of maximum impact lift coefficient with trim and flight-path angle. The data points shown were obtained from faired curves of $C_{L,max}$ plotted against γ_o (samples of which are shown in fig. 8(a)) and the variations shown are faired through these data for γ_o = 5.5°, 10°, 15°, and 20° at C_Δ = 19.15.

Comparison Between Loads of Inverted-V Model and Flat-Bottom Model

Impact-loads data for a flat-bottom model were obtained from tests made under conditions similar to the present investigation and reported in reference 1. These loads for the flat-bottom model are compared with those of the inverted-V model in figure 15 wherein are shown the variations with trim angle of the ratio of the maximum loads for the inverted-V model to the maximum loads for the flat-bottom model. This comparison is limited to low flight-path angles (γ = 10° and below) for trim angles below 30° as the model of reference 1 was of insufficient length to obtain data at high flight-path angles and low trim angles.

The variation shown (fig. 15) indicates that the inverted-V model yields maximum impact loads significantly larger than those of the flat-bottom model (as much as 18 percent at τ = 12°, γ_o = 10°). The variation also shows that, as the severe condition of zero trim or flat impact (impact on a wave flank whose slope angle is equal to the trim angle of a hydro-ski) is approached, the inverted-V model shows a trend toward smaller loads relative to the flat-bottom model. This trend indicates that the inverted-V model, when compared with the flat-bottom model, shows promise as a means of reducing the impact loading under the severe conditions of flat impact without corresponding reduction of load at the less severe conditions of impact at positive trim. Also, at very high trim angles the trend is toward relatively less load for the inverted-V model. However, at these high trim angles the impact loads are mild and the gradual reduction of load shown is of little importance.

Bottom Pressures

Typical distributions of the hydrodynamic pressure on the bottom of the model and maximum values of these pressures are shown in figures 16, 17, and 18.

Figure 16 presents the pressures indicated at each of the gage locations at values of t corresponding to peak readings of each pressure gage for impacts 23, 25, and 29 ($C_\Delta = 19.15$ and $\tau = 8^\circ$). The pressure distribution is shown along with the wetted portion of the model as determined from the water line based on draft measurements and level water.

In figure 17 the variations of maximum pressure (from table II) with $\frac{1}{2}\rho V_n^2$ are presented for trim angles of 4°, 12°, 20°, and 30°. Only the three pressure gages with the highest reading for each trim angle were used and straight lines were faired through the data for each trim angle. The slopes of these lines give pressure coefficients based on velocity normal to the keel, $\frac{p_{max}}{\frac{1}{2}\rho V_n^2}$. The coefficients are converted into an equivalent planing velocity form by dividing by $\sin^2\tau$:

$$\frac{p_{max}}{\frac{1}{2}\rho\left(\frac{V_n}{\sin\tau}\right)^2} = \frac{p_{max}}{\frac{1}{2}\rho \dot{f}^2}$$

The variation with trim angle of these pressure coefficients for the inverted-V model is shown in figure 18 together with pressure coefficients for the flat-bottom model obtained from data of reference 6. Comparison of the peak pressure coefficient for the inverted-V model with that for the flat-bottom model shows that the maximum pressures are approximately the same at trim angles near 21°. Above 21° the inverted-V model experiences somewhat greater pressures (15 percent at 30° trim angle). At trim angles below 21°, the trend of the flat-plate data is not clearly established; however, the pressures for the inverted-V model lie considerably below those for the flat-bottom model. This trend of the maximum pressure lends support to the previous indication that when compared with the flat bottom the inverted-V transverse shape is a means of reducing the impact loading experienced during severe landings at low trims without corresponding reduction of load at the less severe conditions of high trims.

General Observations on the Inverted-V Transverse Shape

From the data presented it has been shown that the impact loads on the inverted-V model were smoothly applied and that, when the maximum loads of the inverted-V model are compared with flat-bottom-model loads, a reduction in load is indicated for landing conditions near flat impact (0° trim). The smooth application of load during impact and the favorable comparison with the loads of the flat-bottom model indicate advantages for the inverted-V model from the standpoint of impact loads.

The planing characteristics of the inverted-V model are presented in reference 7. The planing lift coefficients shown for the inverted-V model, when compared with those of reference 8 for a flat-bottom model, are observed to be equal or greater than the lift coefficients for the flat-bottom model. The planing lift characteristics shown by the data of reference 7 indicate advantages of the inverted-V shape from the standpoint of high planing lift and low hump speeds during take-off.

In addition to impact and planing characteristics, observations were made of the spray generated by the model during impact. The spray observed during impacts of the inverted-V model was confined behind the model with much less spray to the sides or above than is usually observed with conventional flat- or V-bottom models. It is believed that these spray characteristics show promise in the application of the inverted-V shape in hydro-ski or hull designs where spray must be kept to a minimum because of outboard engine inlets, flaps, or other structures.

These observations are intended to point out the potentials of transverse shapes with negative dead-rise angles for hulls and hydro-skis. The present investigation was confined to a -20° angle of dead rise and no attempts have been made to study effects of transverse shape on other configurations having negative dead-rise angles. Therefore, it is felt that the results obtained from the present investigation indicate that further studies of hydro-ski and hull shapes having negative dead-rise angles should be considered.

CONCLUSIONS

An analysis of experimental data obtained in an impact-basin investigation of a narrow-beam model having an inverted-V transverse shape with a dead-rise angle of -20° leads to the following conclusions:

1. The loads, moments, and motions of the inverted-V model vary with initial flight-path angle and trim in a manner similar to the variations obtained with models having positive dead-rise angles.

2. Maximum impact loads on the inverted-V model are greater than loads obtained under similar conditions on a flat-bottom model over intermediate trim angles of this investigation. However, at low trim angles and at very high trim angles, the trends indicate that the loads are smaller on the inverted-V model than on the flat-bottom model.

3. Maximum pressures for the inverted-V model and the flat-bottom model are approximately the same at trims near 21°. The maximum pressures on the inverted-V model are greater at high trims ($\tau = 30^{\circ}$) and smaller at lower trims (below $\tau = 21^{\circ}$) than those on the flat-bottom model.

Langley Aeronautical Laboratory,
National Advisory Committee for Aeronautics,
Langley Field, Va., May 14, 1958.

REFERENCES

1. McArver, A. Ethelda: Water-Landing Investigation of a Model Having Heavy Beam Loadings and 0° Angle of Dead Rise. NACA TN 2330, 1951.

2. Batterson, Sidney A., and McArver, A. Ethelda: Water Landing Investigation of a Model Having a Heavy Beam Loading and a 30° Angle of Dead Rise. NACA TN 2015, 1950.

3. Edge, Philip M., Jr.: Impact-Loads Investigation of Chine-Immersed Models Having Concave-Convex Transverse Shape and Straight or Curved Keel Lines. NACA TN 3940, 1957.

4. Edge, Philip M., Jr.: Impact-Loads Investigation of Chine-Immersed Model Having a Circular-Arc Transverse Shape. NACA TN 4103, 1957.

5. Batterson, Sidney A.: The NACA Impact Basin and Water Landing Tests of a Float Model at Various Velocities and Weights. NACA Rep. 795, 1944. (Supersedes NACA WR L-163.)

6. Smiley, Robert F.: An Experimental Study of Water-Pressure Distributions During Landings and Planing of a Heavily Loaded Rectangular Flat-Plate Model. NACA TN 2453, 1951.

7. Kimon, Peter M.: The Planing Characteristics of an Inverted V Prismatic Surface With Minus 10 Degrees Dead Rise. Rep. 1076, David Taylor Model Basin, Navy Dept., Mar. 1957.

8. Weinstein, Irving, and Kapryan, Walter J.: The High-Speed Planing Characteristics of a Rectangular Flat Plate Over a Wide Range of Trim and Wetted Length. NACA TN 2981, 1953.

TABLE I.- TOTAL LOADS DATA FROM IMPACT TESTS OF A 4 INVERTED-V MODEL WITH -20° DEAD-RISE ANGLE

Impact	Trim, deg	At contact			At $n_{1,max}$								At $M_{Y,max}$				At z_{max}			At rebound	
		z_o, ft/sec	$\dot{z}_o$, ft/sec	γ_o, deg	t, sec	n_1	F_n, lb	z, ft	l, ft	$\dot{s}$, ft/sec	M_Y, lb-ft	C_L	t, sec	n_1	M_Y, lb-ft	C_m	t, sec	n_1	z, ft	t, sec	$\dot{z}$, ft/sec
C_Δ = 19.15																					
1	0	3.6	0	90	0.033	0.97	962	0.11	(a)	3.0	5,192	9k.73	0.033	0.97	5,192	k16	(b)	(b)	(b)	(b)	(b)
2		5.3	0	90	.023	1.81	1,790	.12	(a)	4.3	11,0k2	78.k3	.030	1.08	11,0k2	323	(b)	(b)	(b)	(b)	(b)
3		7.1	0	90	.011	k.89	3,03k	.06	(a)	5.6	18,210	118.31	.027	1.97	18,210	302	(b)	(b)	(b)	(b)	(b)
k		8.9	0	90	.009	7.07	k,161	.07	(a)	7.k	25,902	13.58	.008	7.07	26,29k	3k7	(b)	(b)	(b)	(b)	(b)
5		11.7	0	90	——	——	——	——	(a)	——	——	——	——	——	——	——	(b)	(b)	(b)	(b)	(b)
6	8	3.9	0	90	0.12k	0.16	217	0.33	2.37	3.k	k60	12.62	——	——	——	——	0.7kk	0.16	1.51	(c)	(c)
7		5.7	0	90	.113	.32	368	.91	6.52	k.8	1,033	12.95	.1k3	.28	1,k06	k9	.70k	.17	1.90	(c)	(c)
8		7.k	0	90	.088	.56	687	.61	k.k0	6.k	1,321	12.k6	.198	.kk	2,737	51	.618	.26	2.10	(c)	(c)
9		9.k	0	90	.090	.85	1,08k	.k6	3.31	7.7	2,816	11.63	.138	.68	k,697	63	.603	.26	2.k1	(c)	(c)
10		12.1	0	90	.08k	1.k6	1,921	.90	6.kk	9.5	5,590	12.23	.105	1.12	7,678	5k	.725	.22	2.85	(c)	(c)
11	k	3.9	66.7	3.3k	0.096	0.93	1,309	0.31	k.39	2.0	2,275	.26	0.131	0.69	3,635	0.8k	0.186	0.5k	0.38	0.535	-1.5
12		7.7	67.6	6.53	.066	2.03	2,608	.kk	6.3k	5.0	6,656	.5k	.110	1.33	10,013	2.23	.205	.61	.69	.639	-1.7
13		8.7	62.1	7.99	.06k	2.27	2,9kk	.k6	6.90	6.0	8,2k6	.71	.106	1.39	11,606	3.05	.226	.k6	.82	.758	-1.8
1k		10.k	62.1	9.k6	.057	2.83	3,5k0	.k9	7.07	7.6	9,339	.88	.099	1.73	13,k79	3.51	.229	.36	.87	.766	-2.3
15		10.2	53.5	10.73	.055	2.63	3,363	.k9	7.02	7.8	9,366	1.09	.108	1.3k	12,975	k.52	(b)	(b)	(b)	(b)	(b)
16		8.9	3k.0	1k.65	.065	1.83	2,337	.52	7.38	7.0	6,915	1.82	.122	.87	9,8k8	8.20	(b)	(b)	(b)	(b)	(b)
17		11.6	k3.9	1k.85	.053	3.0k	3,80k	.53	7.60	8.6	10,996	1.82	.112	1.22	16,035	8.0k	(b)	(b)	(b)	(b)	(b)
18		8.5	27.5	17.21	.065	1.55	1,991	.k8	6.9k	6.7	5,975	2.32	.125	.78	8,618	10.75	(b)	(b)	(b)	(b)	(b)
19		8.0	2k.9	17.80	.068	1.37	1,698	.k8	6.9k	6.k	5,00k	2.k7	.126	.69	6,910	10.kk	(b)	(b)	(b)	(b)	(b)
20	12	3.9	79.k	2.78	0.099	1.26	1,792	0.30	2.16	1.k	2,006	0.25	0.131	1.07	3,385	0.55	0.139	1.11	0.32	0.315	-2.k
21		3.9	73.0	3.05	.11k	1.18	1,537	.32	2.26	1.3	2,1k3	.27	.13k	1.20	3,598	.70	.1k9	.97	.32	.338	-2.6
22		7.3	67.6	6.11	.091	1.89	2,506	.k9	3.52	3.5	k,178	.51	.107	1.6k	6,39k	1.k3	.162	.98	.58	.k23	-3.2
23		9.3	61.k	8.6k	.08k	2.39	3,19k	.63	k.51	5.2	6,292	.77	.110	1.78	9,063	2.k3	.175	1.26	.81	.507	-3.5
(d)		11.1	60.9	10.29	.079	2.90	3,853	.69	k.96	6.3	8,551	.93	.105	2.17	12,008	3.2k	.176	1.30	.92	.528	-3.7
2k		10.9	55.6	11.10	.063	2.60	3,k01	.62	3.11	7.9	7,139	1.03	.111	1.75	10,876	3.50	.201	.89	1.01	.612	-3.2
25		11.3	k6.7	13.58	.079	2.6k	3,k47	.73	5.25	7.1	7,956	1.k1	.103	2.05	12,206	5.k5	.203	.91	1.11	.7k0	-3.0
26		11.2	kk.3	14.25	.052	2.57	3,165	.5k	3.87	8.6	6,520	1.52	.112	1.52	10,790	5.3k	.257	.72	1.20	.812	-2.6
27		12.1	k0.0	16.88	.076	2.55	3,359	.77	5.53	7.8	7,501	1.80	.106	1.7k	12,51k	7.39	.296	.53	1.30	.910	-2.6
28		10.9	3k.5	17.60	.080	2.09	2,8k3	.76	5.k6	7.5	6,778	1.97	.108	1.50	9,731	7.67	.313	.kk	1.38	1.099	-1.8
29		11.9	32.7	20.06	.079	2.k3	3,1k5	.79	5.68	8.1	7,k76	2.k8	.107	1.62	11,831	10.05	.327	.32	1.k5	1.137	-1.9
30		9.6	25.6	20.57	.08k	1.k9	1,992	.72	5.07	7.0	k,598	2.kk	.109	1.18	6,727	9.25	.399	.30	1.k8	1.k82	-1.3
31		11.0	28.k	21.15	.082	2.01	2,652	.78	5.61	7.7	6,879	2.68	.108	1.57	10,751	11.96	.383	.3k	1.55	1.27k	-1.6
32	12	3.9	73.0	3.06	0.10k	1.27	1,801	0.32	1.52	1.2	1,587	0.29	0.122	1.25	2,695	0.52	0.1k2	1.12	0.33	0.30k	-2.7
33		6.2	61.k	5.81	.095	1.65	2,321	.k6	2.20	3.3	3,855	.5k	.132	1.36	k,777	1.30	.15k	1.13	.52	.372	-3.6
3k		9.3	51.0	10.35	.089	2.15	2,902	.69	3.33	5.k	5,6k4	.99	.119	1.69	7,535	2.89	.189	1.15	.91	.520	-3.9
35		11.5	k2.k	15.13	.088	2.38	3,155	.81	3.89	7.1	7,178	1.52	.108	1.95	9,6k3	5.17	.2k3	.76	1.21	.690	-3.6
36		11.9	33.3	19.62	.082	2.10	2,778	.83	3.96	8.1	6,073	2.07	.120	1.k7	8,k26	6.95	.295	.6k	1.k5	.937	-2.7
37		8.6	18.7	2k.76	.092	.95	1,2k3	.70	3.38	7.0	2,619	2.75	.137	.81	3,871	9.39	.k77	.30	1.65	(e)	(e)
38	16	k.k	80.0	3.15	0.110	1.75	2,k35	0.30	1.09	0.6	2,56k	0.3k	0.137	1.50	3,105	0.50	0.112	1.73	0.30	0.239	-3.6
39		6.3	62.1	5.82	.103	1.68	2,306	.k9	1.78	3.1	3,36k	.53	.132	1.k7	k,82k	1.28	.155	1.28	.55	.360	-3.9
k0		9.5	51.0	10.58	.092	2.22	3,037	.71	2.57	5.3	5,08k	1.02	.122	1.78	6,562	2.51	.17k	1.51	.89	.kk8	-k.8
k1		11.5	k3.1	1k.99	.090	2.37	3,19k	.8k	3.06	6.9	5,973	1.k7	.120	1.90	7,957	k.13	.222	.99	1.18	.587	-k.6
k2		7.k	2k.6	16.72	.095	.91	1,285	.65	2.3k	5.8	2,k29	1.69	.212	.69	3,036	k.7k	.368	.kk	1.29	1.167	-1.7
k3		12.2	32.9	20.32	.089	2.13	2,900	.93	3.38	8.3	6,107	2.73	.130	1.k1	6,2k1	5.2k	.26k	.91	1.51	.825	-3.6
kk	20	3.2	73.5	2.k6	0.121	1.32	1,89k	0.2k	0.71	0.6	2,102	0.30	0.138	1.25	2,731	0.52	0.118	1.33	0.25	0.2kk	-2.7
k5		k.3	67.6	3.62	.11k	1.57	2,199	.3k	1.00	.9	2,302	.k1	.123	1.57	3,120	.70	.129	1.50	.36	.276	-3.7
k6		6.2	62.1	5.66	.105	1.90	2,6k9	.k7	1.38	2.5	3,791	.60	.128	1.69	k,513	1.20	.1k3	1.57	.50	.308	-k.5
k7		7.9	k6.3	9.65	.100	1.7k	2,k66	.65	1.89	k.k	k,385	.97	.137	1.53	k,802	2.25	.187	1.31	.81	.k51	-k.6
k8		8.0	k3.5	10.k8	.101	1.62	2,36k	.66	1.92	k.8	k,678	1.02	.177	1.38	5,8kk	3.09	.197	1.17	.85	.k9k	-k.5
k9		9.7	33.8	15.96	.101	1.k7	2,013	.81	2.38	6.k	3,36k	1.k7	.126	1.39	k,k88	3.75	.261	.83	1.2k	.705	-3.9
50		6.8	21.6	17.61	.1k5	.69	919	.85	2.k8	5.6	2,2k7	1.63	.210	.69	2,799	5.66	.k10	.35	1.36	1.297	-1.k
51		12.0	33.9	19.51	.093	2.09	2,936	.96	2.81	8.1	6,307	1.99	.123	1.78	7,510	5.99	.258	.98	1.50	.727	-k.3
52		7.5	19.2	21.36	.1k8	.73	878	.9k	2.75	k.3	2,163	1.87	.178	.73	2,787	6.75	.kk8	.30	1.57	1.5k2	-1.0
53		11.2	28.6	21.k8	.09k	1.58	2,2k0	.89	2.60	8.0	k,523	2.06	.128	1.k5	6,189	6.77	.308	.65	1.60	1.018	-3.5
5k	30	k.5	67.6	3.80	0.118	1.80	2,6k5	0.35	0.70	0.5	3,k25	0.k8	0.13k	1.72	3,k86	0.78	0.117	1.80	0.35	0.2k8	-k.3
55		7.5	52.9	8.05	.106	1.92	2,861	.60	1.20	3.3	k,259	.83	.121	1.86	5,007	1.81	.156	1.69	.65	.336	-5.7
56		8.6	k8.1	10.08	.103	2.01	2,973	.71	1.k1	k.7	k,531	1.0k	.131	1.87	k,907	2.12	.171	1.71	.83	.393	-6.2
57		10.6	k0.0	1k.79	.105	1.88	2,739	.91	1.82	6.2	k,792	1.35	.130	1.79	5,78k	3.k9	.215	1.38	1.22	.527	-6.2
58		12.2	33.6	19.95	.099	1.90	2,86k	1.03	2.06	8.3	5,235	1.8k	.16k	1.76	5,876	k.79	.251	1.20	2.57	.653	-5.8
59		8.7	20.3	23.28	.163	.85	1,276	1.18	2.36	5.1	2,965	2.1k	.193	.85	3,360	7.12	.k38	.k0	1.80	1.315	-2.k
C_Δ = 27.90																					
60	8	k.5	71.k	3.57	0.103	0.85	1,7k6	0.38	2.72	3.1	2,703	0.29	0.1k0	0.85	k,605	0.93	0.211	0.73	0.51	0.k96	-2.6
61		7.7	65.8	6.68	.098	1.66	3,287	.62	k.k6	k.5	8,139	.68	.116	1.5k	11,220	2.6k	.215	.81	.8k	.603	-2.8
62		8.1	kk.6	10.26	.096	1.k0	2,715	.68	k.87	5.k	7,768	1.23	.116	1.29	10,870	5.k5	.306	.k9	1.13	.956	-2.1
63		12.k	37.9	18.06	.08k	2.09	k,007	.89	6.k2	8.5	12,870	2.37	.11k	1.50	17,002	11.06	(b)	(b)	(b)	(b)	(b)
6k		12.k	33.3	20.k1	.085	1.99	3,8k1	.90	6.k8	8.5	12,802	2.82	.105	1.68	17,399	1k.20	(b)	(b)	(b)	(b)	(b)
C_Δ = 36.07																					
65	8	5.8	72.5	k.55	0.122	0.86	2,213	0.k6	3.33	2.k	k,632	0.38	0.1k7	0.80	9,021	1.73	0.222	0.62	0.56	0.570	-2.0
66		5.9	63.3	5.29	.107	1.12	2,859	.56	3.87	3.7	8,03k	.6k	.1k0	.89	9,610	2.5k	.255	.k8	.76	.666	-2.5
67		7.7	kk.3	9.92	.100	.99	2,588	.69	k.96	5.7	8,113	1.1k	.1k5	.76	9,185	k.75	.390	.31	1.31	1.262	-1.k
68		9.8	36.8	1k.85	.087	1.26	3,029	.75	5.k2	7.2	9,950	2.02	.131	.91	12,991	9.27	(b)	(b)	(b)	(b)	(b)
69		12.1	k1.7	16.2k	.086	2.11	k,058	.87	6.27	8.1	1k,309	2.60	.116	1.5k	19,560	10.71	(b)	(b)	(b)	(b)	(b)
70		11.6	31.3	20.k1	.091	1.36	3,512	.92	6.61	8.6	12,k57	2.8k	.139	1.10	1k,517	13.0k	(b)	(b)	(b)	(b)	(b)

[a]Full length, 12 feet.
[b]Nose of the model became immersed prior to maximum draft.
[c]No exit from water.
[d]Average of six repeat impacts.

TABLE II.- MAXIMUM PRESSURE AND INSTANTANEOUS VERTICAL-VELOCITY DATA

Impact	Trim, deg	γ_o, deg	$\dot{x}_o$, ft/sec	Gage 1		2		3		4		5		6		7		8		9		10	
				$\dot{z}$, ft/sec	p_{max}	$\dot{z}$, ft/sec	p_{max}	$\dot{z}$, ft/sec	p_{max}	$\dot{z}$, ft/sec	p_{max}	$\dot{z}$, ft/sec	p_{max}	$\dot{z}$, ft/sec	p_{max}	$\dot{z}$, ft/sec	p_{max}	$\dot{z}$, ft/sec	p_{max}	$\dot{z}$, ft/sec	p_{max}	$\dot{z}$, ft/sec	p_{max}
C_Δ = 19.15																							
1 to 4	0	90	0	----	----	----	----	----	----	----	----	----	----	----	----	----	----	----	----	----	----	----	----
5	0	90	0	11.5	15.4	----	----	----	----	11.3	10.7	11.7	8.2	11.8	11.0	11.8	9.2	11.8	8.6	----	----	11.7	6.3
6		90	0	3.9	1.9	----	----	----	----	3.4	6.6	3.4	7.1	3.2	5.4	3.2	5.8	3.1	2.3	----	----	----	----
7		90	0	5.5	7.7	----	----	----	----	5.5	2.5	5.3	2.4	4.8	21.2	4.8	6.8	4.8	5.9	----	----	----	----
8	8	90	0	7.4	9.6	----	----	----	----	7.4	5.8	7.0	13.5	6.7	4.3	6.5	7.7	6.4	9.5	----	----	----	----
9		90	0	9.3	19.2	----	----	----	----	9.2	11.6	9.0	20.6	----	----	8.0	10.1	8.2	15.8	----	----	7.6	11.4
10		90	0	12.1	37.1	----	----	----	----	12.1	14.9	11.7	27.7	11.2	18.4	10.6	10.1	10.8	22.1	----	----	----	----
11		3.34	66.7	3.6	5.3	----	----	2.7	6.3	2.7	4.3	2.7	22.3	1.8	19.0	----	----	1.1	7.7	----	----	----	----
12		6.53	67.6	7.6	39.8	7.5	17.8	7.5	11.8	7.6	15.3	7.1	59.1	6.5	53.3	5.6	22.7	5.9	18.7	6.5	3.8	4.4	6.5
13		7.99	62.1	8.8	52.0	8.6	17.0	8.9	12.6	8.6	22.4	8.1	52.4	7.7	59.1	6.8	23.5	6.8	19.9	6.8	6.9	6.0	17.8
14		9.46	62.1	10.1	54.5	10.0	12.0	10.1	17.7	10.0	27.8	9.6	79.6	9.3	45.9	8.6	31.5	8.6	24.5	9.2	5.3	7.7	13.0
15	4	10.73	53.5	10.0	46.2	9.9	26.0	10.1	14.9	9.9	25.6	9.6	68.5	9.1	37.1	8.4	24.8	8.5	22.3	9.0	3.4	7.8	8.7
16		11.65	54.0	9.0	25.8	8.9	22.9	9.0	13.2	9.0	19.1	8.6	35.3	8.2	44.4	7.7	14.8	7.8	16.9	----	----	7.0	11.8
17		14.85	43.9	11.2	49.3	----	----	11.3	17.7	11.2	28.7	10.9	51.6	10.3	71.9	9.8	39.9	9.8	24.8	10.1	4.7	9.2	20.0
18		17.21	27.5	8.5	25.6	8.4	22.2	8.4	7.0	8.3	13.6	8.1	36.2	7.7	44.3	7.2	13.2	7.4	15.0	7.2	4.3	6.7	9.9
19		17.80	24.9	8.0	21.7	7.9	10.0	7.9	10.5	7.9	17.9	7.7	38.4	7.3	46.2	6.8	22.8	6.9	15.7	7.2	2.4	6.3	9.1
20		2.78	79.4	3.7	25.7	----	----	----	----	3.3	29.8	----	0	----	0	----	0	----	0	----	0	----	0
21		3.05	73.0	3.7	23.6	----	----	3.6	15.8	3.3	25.1	----	----	----	0	----	----	----	----	----	0	----	0
22		6.14	67.6	7.2	40.6	----	----	7.1	17.3	7.0	30.0	5.7	39.7	3.8	29.3	----	0	----	0	----	0	----	0
23		8.64	61.4	9.2	69.4	9.0	17.7	9.1	22.4	9.1	39.2	8.1	29.6	6.5	30.0	4.8	24.7	5.1	34.0	5.4	12.0	2.3	9.6
(a)		10.29	60.9	10.9	57.7	10.6	24.2	10.9	62.6	10.8	37.3	9.8	26.5	8.6	42.9	6.8	26.6	7.1	39.5	7.3	9.9	4.2	12.3
24		11.10	55.6	10.8	48.5	10.5	24.7	10.8	34.3	----	----	9.8	39.9	8.8	46.2	7.4	16.2	----	----	----	----	----	----
25	8	13.58	46.7	11.3	62.2	11.0	21.8	11.2	24.3	11.2	37.9	10.2	51.6	9.3	42.6	7.8	18.8	8.2	32.6	8.3	5.7	5.9	8.6
26		14.25	44.3	11.2	62.2	11.0	26.2	11.1	34.0	----	----	10.2	52.2	11.0	44.7	8.0	20.7	----	----	----	----	----	----
27		16.88	40.0	12.1	54.4	----	----	12.0	21.7	11.9	30.3	11.3	39.3	10.4	33.4	9.1	22.7	9.2	28.8	----	----	7.7	21.0
28		17.60	34.5	10.9	43.6	----	----	10.9	33.7	----	----	10.0	48.1	8.7	28.3	----	----	----	----	----	----	----	----
29		20.06	32.7	12.0	56.2	11.9	27.8	12.0	15.9	11.9	32.1	11.4	60.7	10.5	36.7	9.3	12.2	9.6	30.4	9.8	11.5	8.2	11.3
30		20.57	25.6	9.5	35.2	9.5	16.7	9.5	16.9	9.5	25.2	8.9	25.4	8.3	20.6	7.4	11.8	7.5	18.4	7.7	8.2	6.2	5.1
31		21.15	28.4	11.0	55.5	----	----	10.9	29.1	10.9	18.8	10.3	27.2	9.5	15.6	8.7	21.2	9.0	22.5	----	----	7.6	13.9
32		3.08	73.0	3.5	28.8	----	----	2.9	33.9	2.4	45.9	----	0	----	0	----	0	----	0	----	0	----	0
33		5.81	61.4	6.2	29.4	----	----	5.8	33.2	5.6	39.0	3.0	8.5	----	0	----	----	----	----	----	0	----	0
34	12	10.35	51.0	9.1	32.5	----	----	9.1	29.5	8.9	43.3	7.7	16.2	5.6	36.3	2.1	6.5	2.6	17.4	2.7	5.6	0.4	1.4
35		15.13	43.1	11.5	37.5	----	----	11.3	28.9	11.2	39.5	9.9	8.3	8.4	37.1	6.0	12.6	6.5	25.6	6.6	9.2	3.8	7.4
36		19.62	24.6	11.8	29.3	----	----	----	----	11.5	38.8	10.6	11.5	9.1	26.7	7.7	14.9	7.9	24.7	8.0	9.5	5.7	5.8
37		24.76	32.9	8.4	14.0	----	----	8.4	11.8	8.4	19.4	7.8	5.0	6.8	18.8	6.0	3.8	6.1	13.2	6.2	3.4	4.9	2.1
38		3.15	80.0	3.9	41.6	----	----	----	----	1.6	46.9	----	0	----	0	----	----	----	----	----	----	----	----
39		5.82	62.1	6.2	23.5	----	----	----	----	5.1	40.4	----	----	----	0	----	----	----	----	----	----	----	----
40	16	10.58	51.0	9.3	16.7	----	----	9.0	38.0	8.9	45.4	6.8	10.9	2.7	20.3	----	----	----	----	----	----	----	----
41		14.99	43.1	11.4	28.6	----	----	----	----	10.9	44.5	9.2	8.9	6.7	36.7	----	----	----	----	----	----	----	----
42		16.72	24.6	7.3	12.6	----	----	7.1	17.6	7.0	20.6	6.2	5.1	4.5	17.1	----	----	----	----	----	----	----	----
43		20.32	32.9	12.1	28.2	----	----	11.9	28.5	11.9	35.2	10.5	9.3	8.6	32.8	----	----	----	----	----	----	----	----
44		2.46	73.5	2.9	35.9	----	----	----	0	----	0	----	0	----	0	----	0	----	0	----	0	----	0
45		3.62	67.6	3.9	36.4	----	----	1.5	33.6	.9	36.9	----	0	----	0	----	0	----	0	----	0	----	0
46		5.66	62.1	6.1	39.4	----	----	5.0	38.5	4.8	42.9	----	0	----	0	----	0	----	0	----	0	----	0
47		9.65	46.3	7.7	27.6	----	----	7.2	30.3	7.1	36.1	4.1	21.8	----	0	----	----	----	----	----	0	----	0
48	20	10.48	43.5	7.8	23.2	----	----	7.5	25.4	7.4	28.1	4.5	20.7	----	----	----	----	----	----	----	0	----	0
49		15.96	33.8	9.4	19.0	----	----	8.9	24.6	8.9	30.2	7.1	26.3	----	----	----	----	----	----	----	0	----	0
50		17.61	21.6	7.0	8.2	----	----	6.6	13.8	6.5	16.5	5.4	12.7	3.7	4.2	3.1	2.4	3.1	20.7	----	0	----	0
51		19.51	33.9	12.0	25.0	----	----	11.7	32.4	11.6	36.3	10.1	31.1	7.5	27.7	4.5	6.1	----	----	----	----	----	----
52		21.36	19.2	7.3	12.0	----	----	7.1	16.8	7.1	17.1	6.2	10.7	5.0	16.0	----	----	----	----	----	----	----	----
53		21.48	28.6	11.2	21.6	----	----	10.6	21.0	10.6	28.9	9.2	26.3	7.1	13.3	4.6	7.7	----	----	----	0	----	0
54		3.80	67.6	4.1	34.2	----	----	----	0	----	0	----	0	----	0	----	----	----	----	----	----	----	0
55		8.05	52.9	7.2	29.7	----	----	5.5	35.1	5.5	36.1	----	0	----	0	----	----	----	----	----	0	----	0
56	30	10.08	48.1	8.3	25.5	----	----	7.9	29.2	7.4	29.7	1.8	6.3	----	0	----	----	----	----	----	0	----	0
57		14.79	40.0	10.2	23.8	----	----	9.5	28.4	9.5	27.3	6.5	16.3	----	----	----	----	----	----	----	0	----	0
58		19.95	33.6	12.1	25.3	----	----	11.6	27.5	11.5	28.5	9.3	19.9	5.5	12.9	----	----	----	----	----	0	----	0
59		23.28	20.3	8.6	10.5	----	----	8.2	14.9	8.1	15.9	6.8	2.9	5.7	6.2	----	----	----	----	1.7	5.4	----	0
C_Δ = 27.90																							
60		3.57	71.4	4.7	29.6	----	----	----	----	3.9	35.3	2.1	23.7	----	----	----	----	----	----	----	----	----	----
61		6.68	65.8	7.5	36.4	----	----	----	----	----	----	6.8	34.5	5.5	32.3	4.0	21.7	4.5	33.8	----	----	----	----
62	8	10.26	44.6	8.1	36.6	----	----	----	----	8.1	17.9	7.6	22.8	7.1	34.0	6.1	24.1	6.2	27.5	----	----	2.2	22.0
63		18.06	37.9	12.4	51.7	----	----	----	----	12.1	27.7	11.6	25.0	11.2	29.7	10.5	31.9	10.6	31.5	----	----	4.8	9.9
64		20.41	33.3	12.5	50.5	----	----	----	----	12.3	27.8	11.9	50.2	11.4	35.7	10.6	24.6	10.8	33.8	----	----	9.4	25.3
																						9.6	23.7
C_Δ = 36.07																							
65		4.55	72.5	4.4	23.1	----	----	----	----	4.1	33.3	3.2	28.1	1.8	16.7	----	----	1.7	16.2	----	0	----	0
66		5.29	63.3	6.0	36.4	----	----	----	----	5.7	24.7	5.3	27.7	4.4	30.5	3.3	17.9	3.6	32.0	----	----	1.9	10.1
67	8	9.92	44.3	7.7	37.0	----	----	----	----	7.8	16.5	7.6	20.1	6.8	22.4	6.1	23.2	6.2	30.6	----	----	5.2	11.6
68		14.85	36.8	9.6	38.6	----	----	----	----	9.4	19.0	9.3	30.7	9.0	17.6	8.0	11.6	8.3	31.1	----	----	7.3	8.3
69		16.24	41.7	12.1	49.1	----	----	----	----	12.0	27.2	11.5	31.8	10.9	22.3	10.1	36.2	10.1	41.0	----	----	9.0	16.4
70		20.41	31.3	11.4	44.0	----	----	----	----	11.1	26.8	10.9	39.6	10.7	27.5	9.8	36.7	9.9	34.2	----	----	9.4	8.1

[a]Average of six repeat impacts.

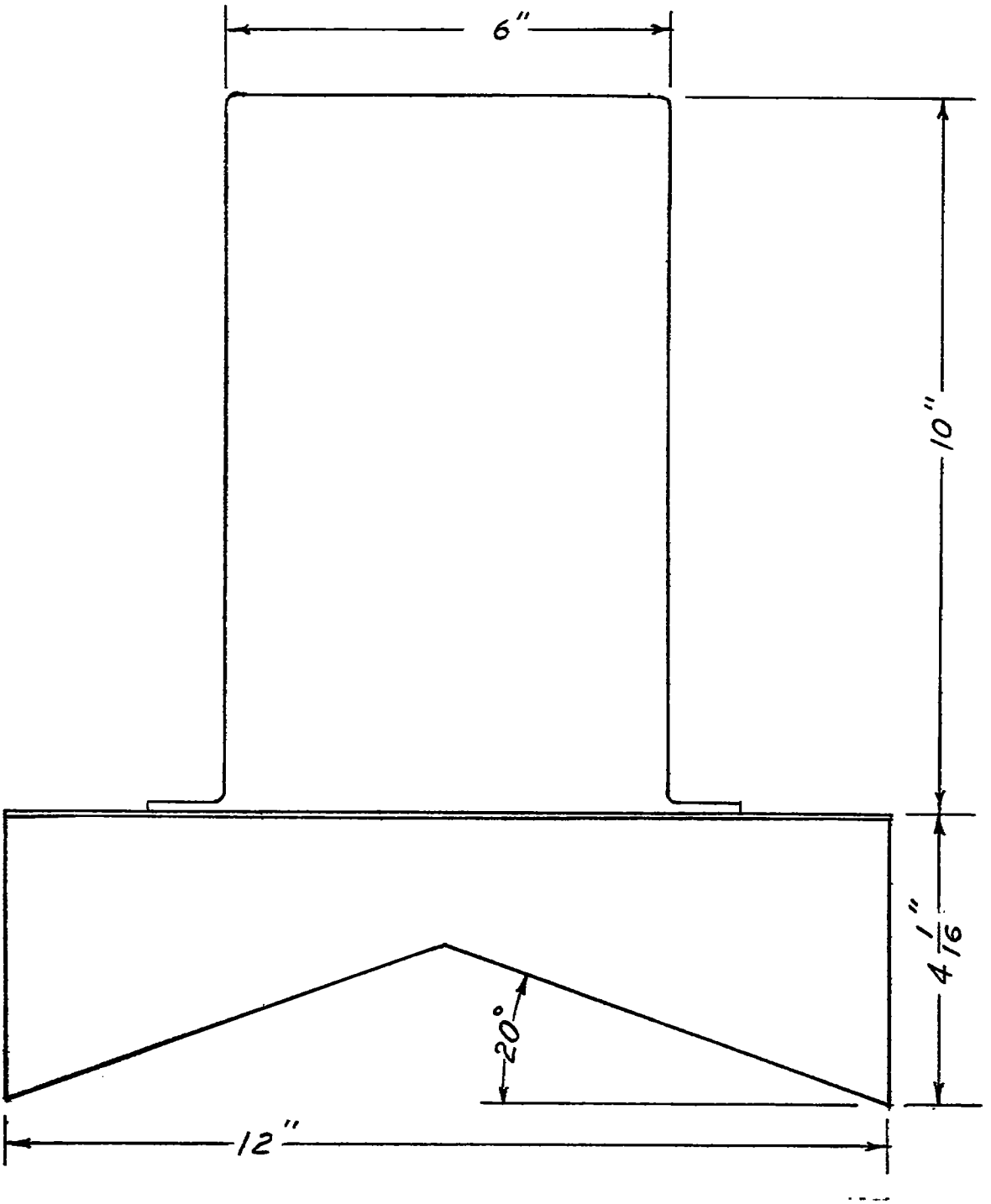

Figure 1.- Cross section of inverted-V model.

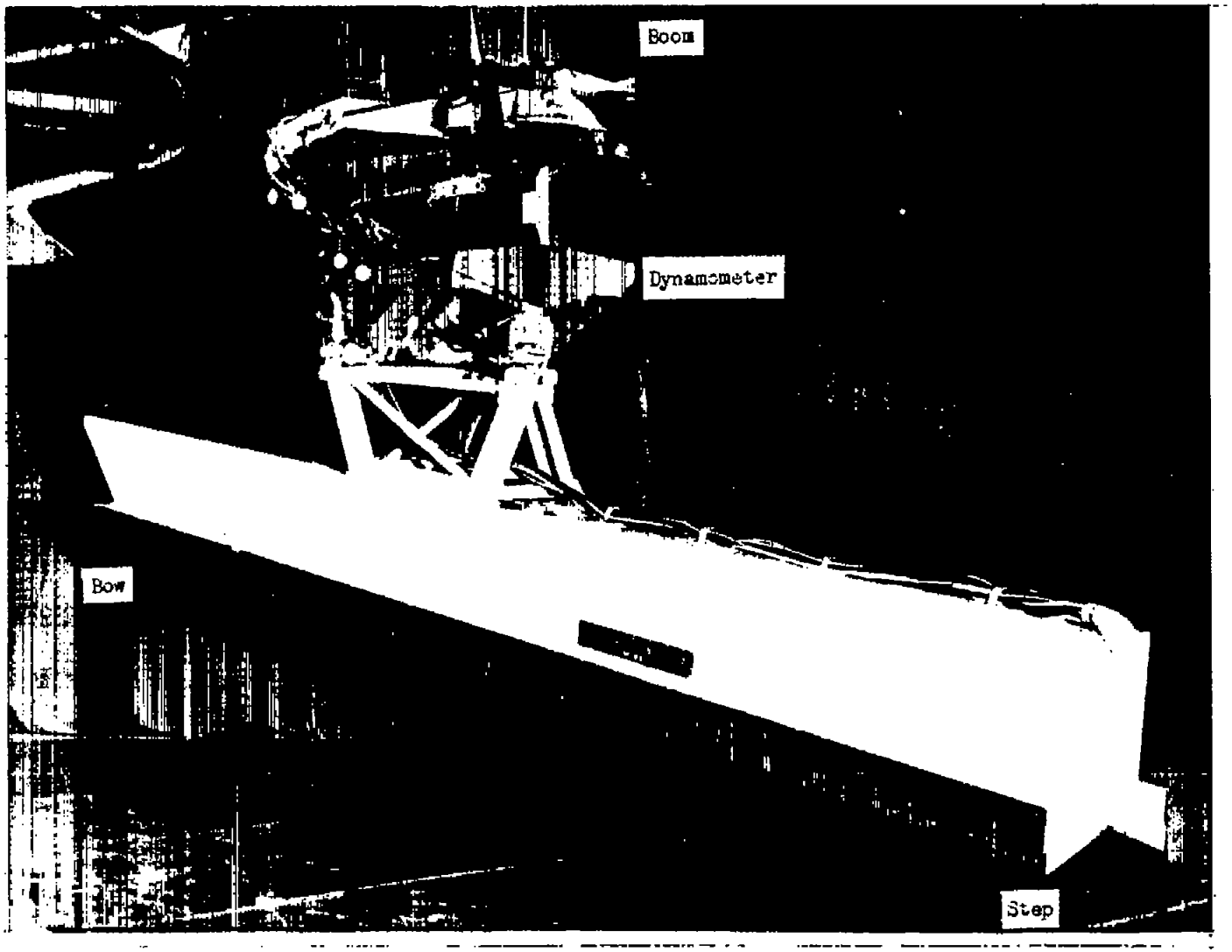

Figure 2.- Inverted-V model mounted on carriage in Langley impact basin. L-93869.1

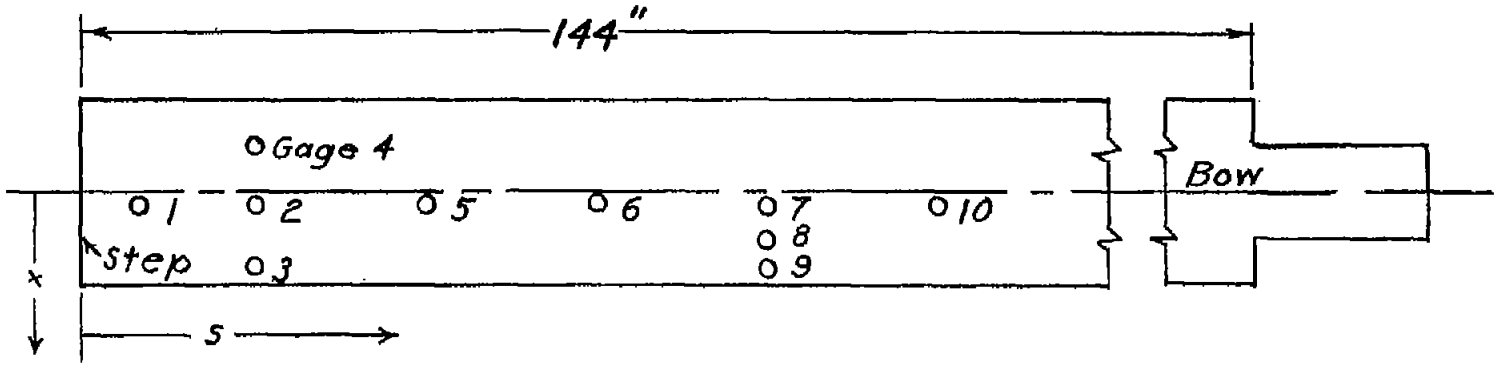

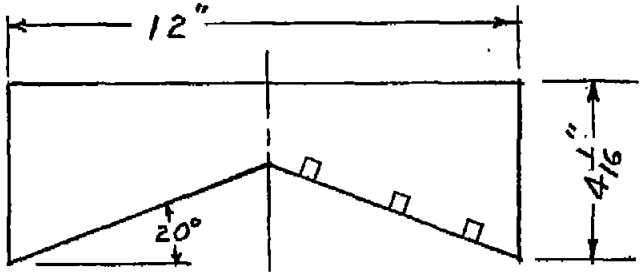

Gage	s, ft	x, ft
1	0.35	0.06
2	1.02	.06
3	1.02	.39
4	1.02	.24
5	2.02	.06
6	3.02	.06
7	4.02	.06
8	4.02	.24
9	4.02	.39
10	5.02	.06

Figure 3.- Locations of pressure gages in bottom of inverted-V model having -20° angle of dead rise.

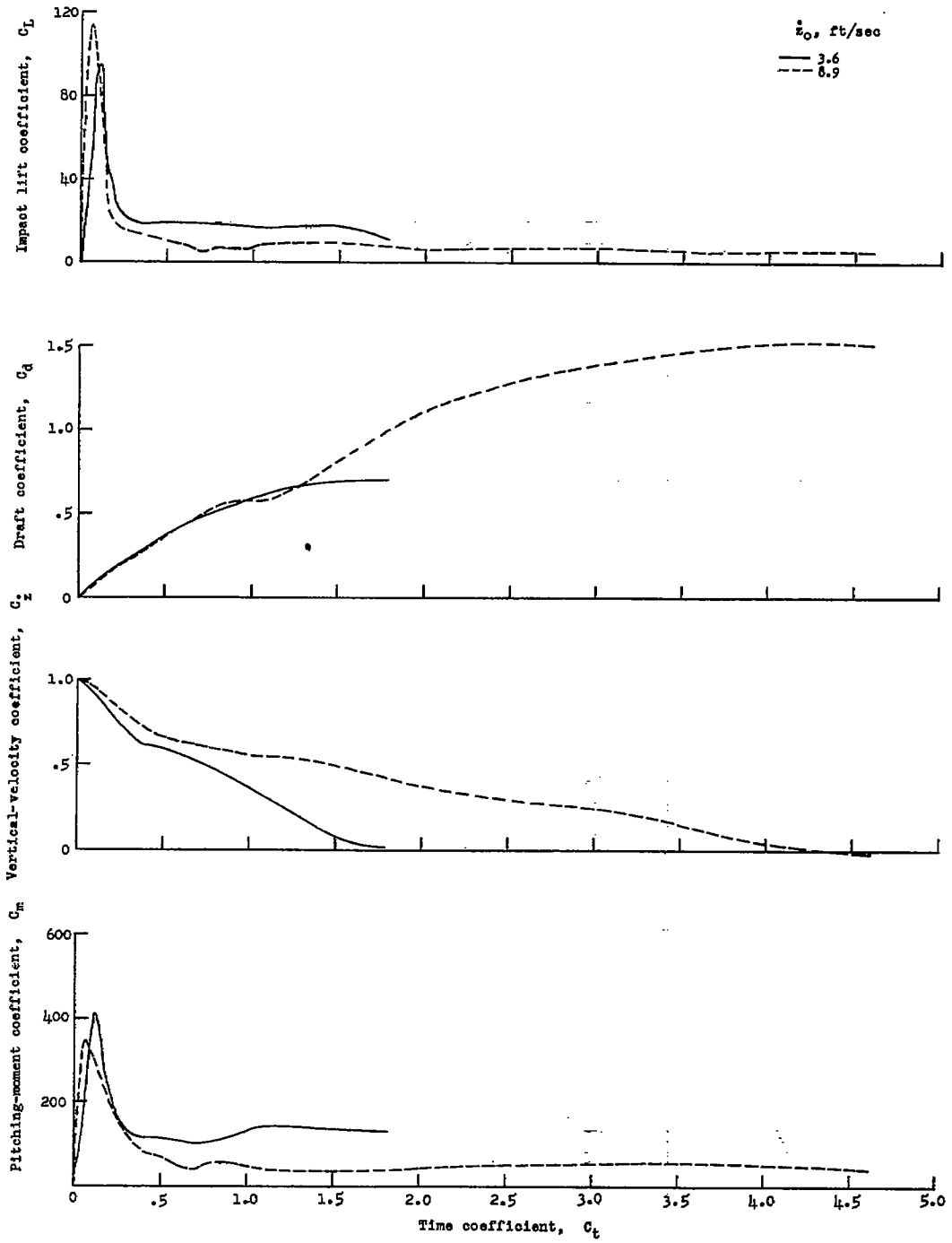

Figure 4.- Variations of load and motion coefficients with time coefficient for impacts without forward speed. $\tau = 0^o$; $C_\Delta = 19.15$.

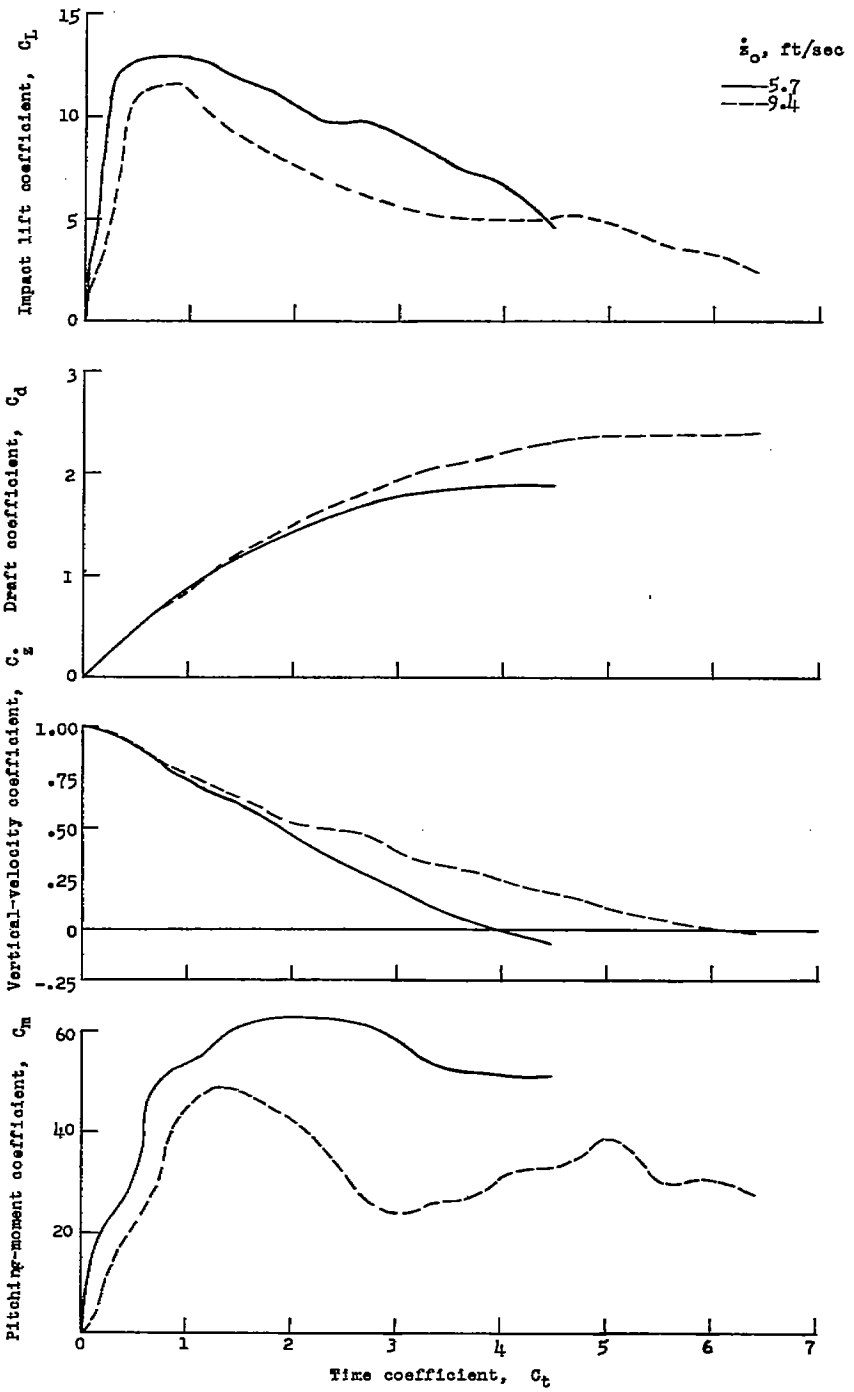

Figure 5.- Variations of load and motion coefficients with time coefficient for impacts without forward speed. $\tau = 8^{\circ}$; $C_{\Delta} = 19.15$.

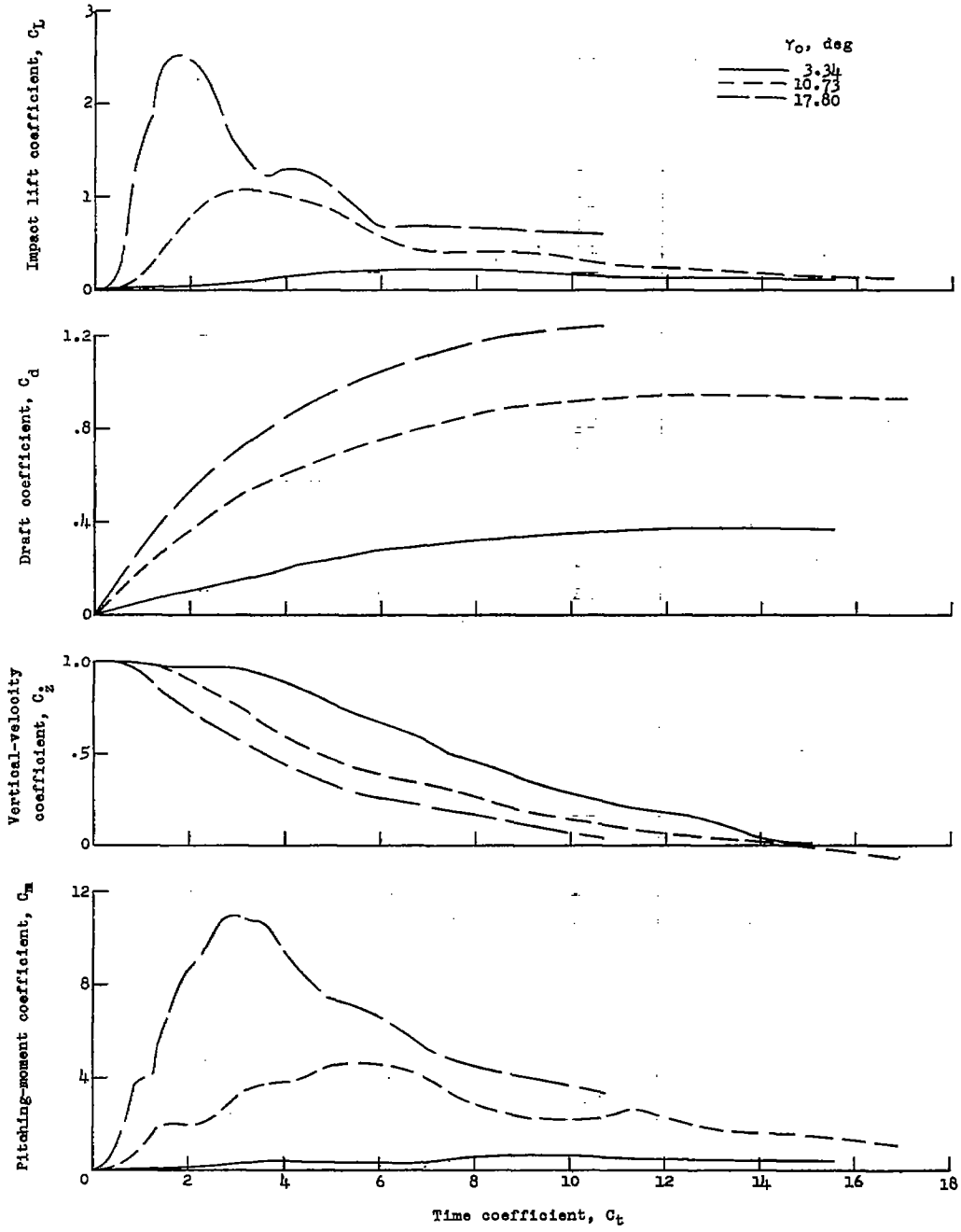

(a) $\tau = 4^o$.

Figure 6.- Variations of the load and motion coefficients with time coefficient for impacts with forward speed. $C_\Delta = 19.15$.

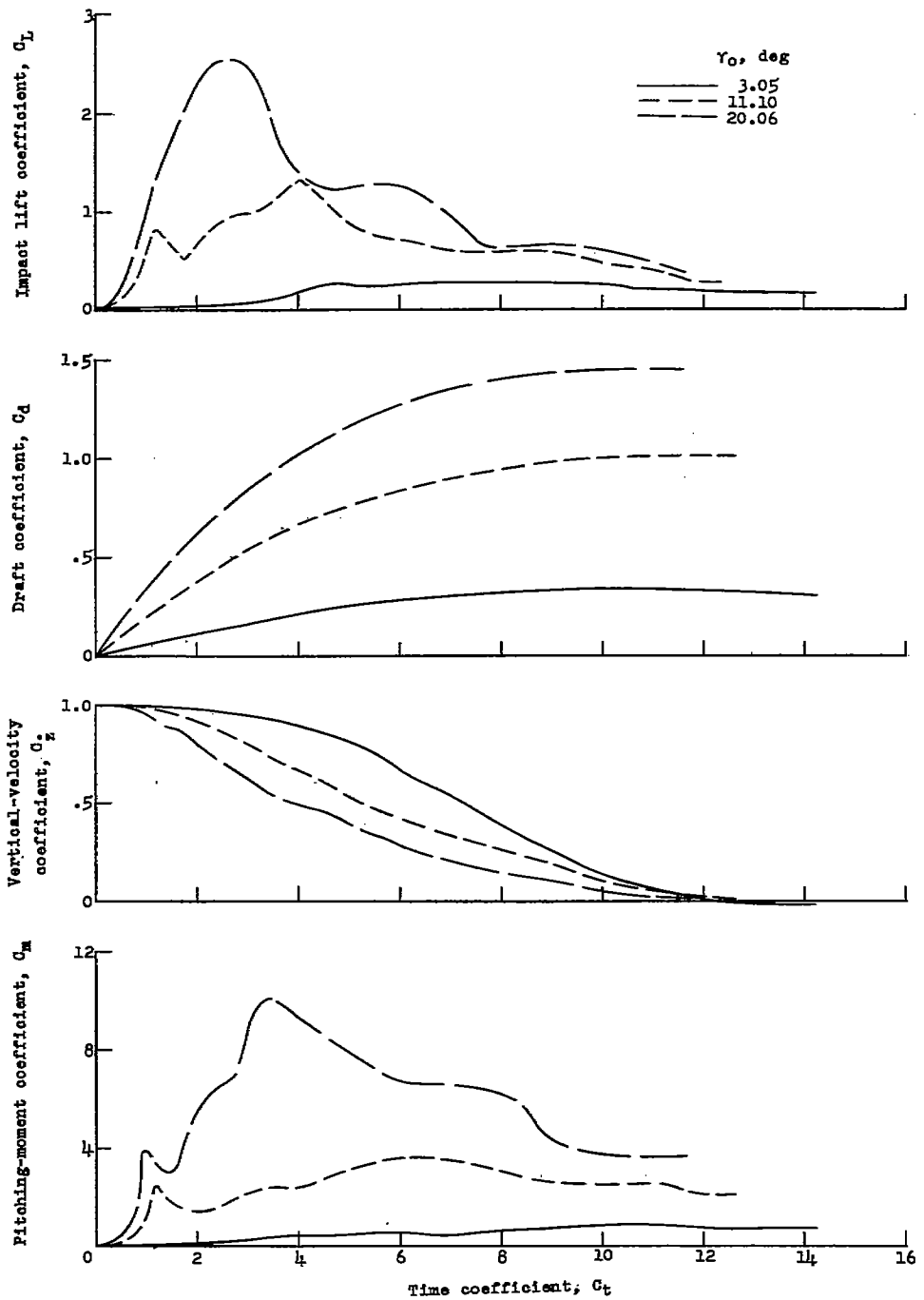

(b) $\tau = 8^o$.

Figure 6.- Continued.

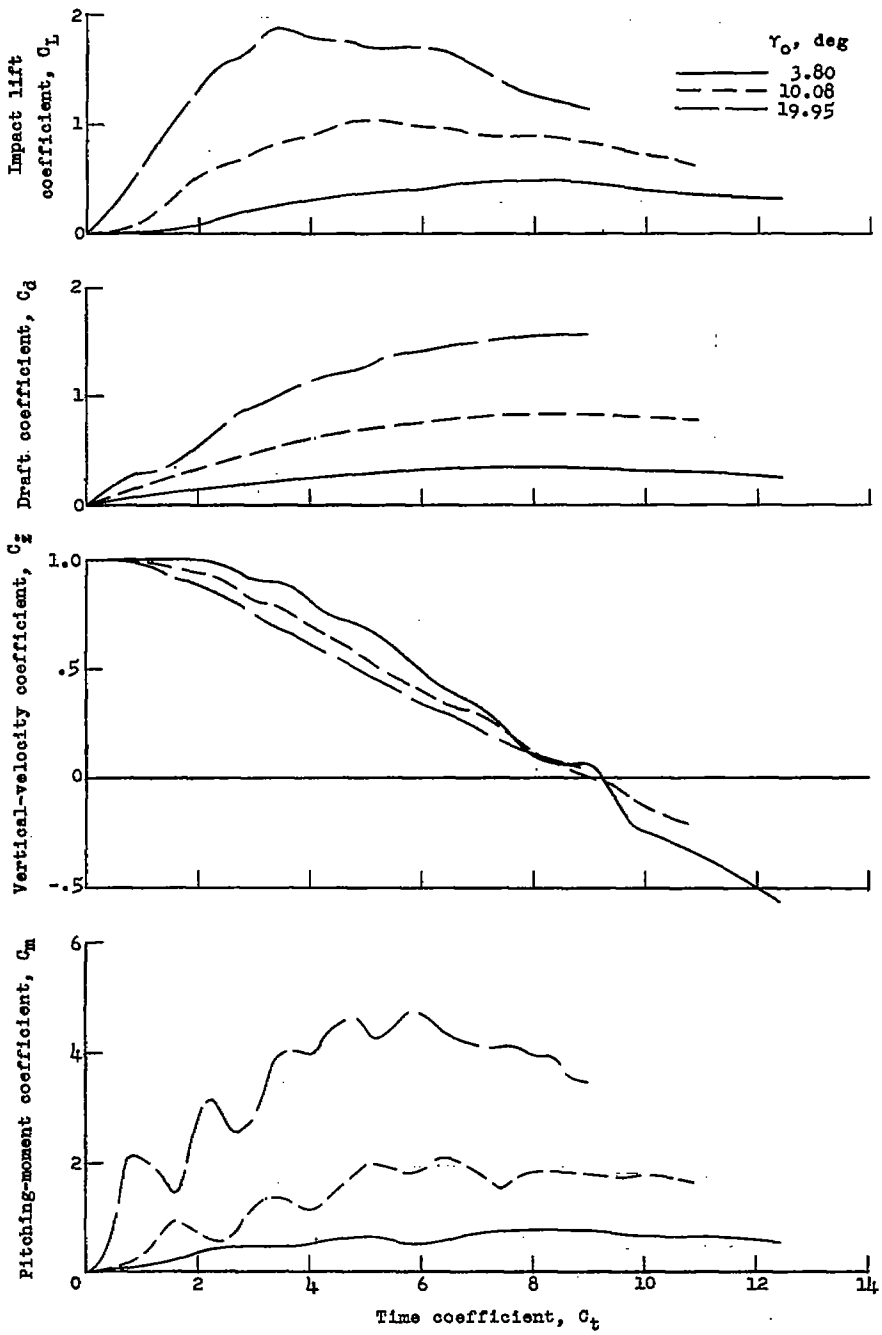

(c) $\tau = 30^\circ$.

Figure 6.- Concluded.

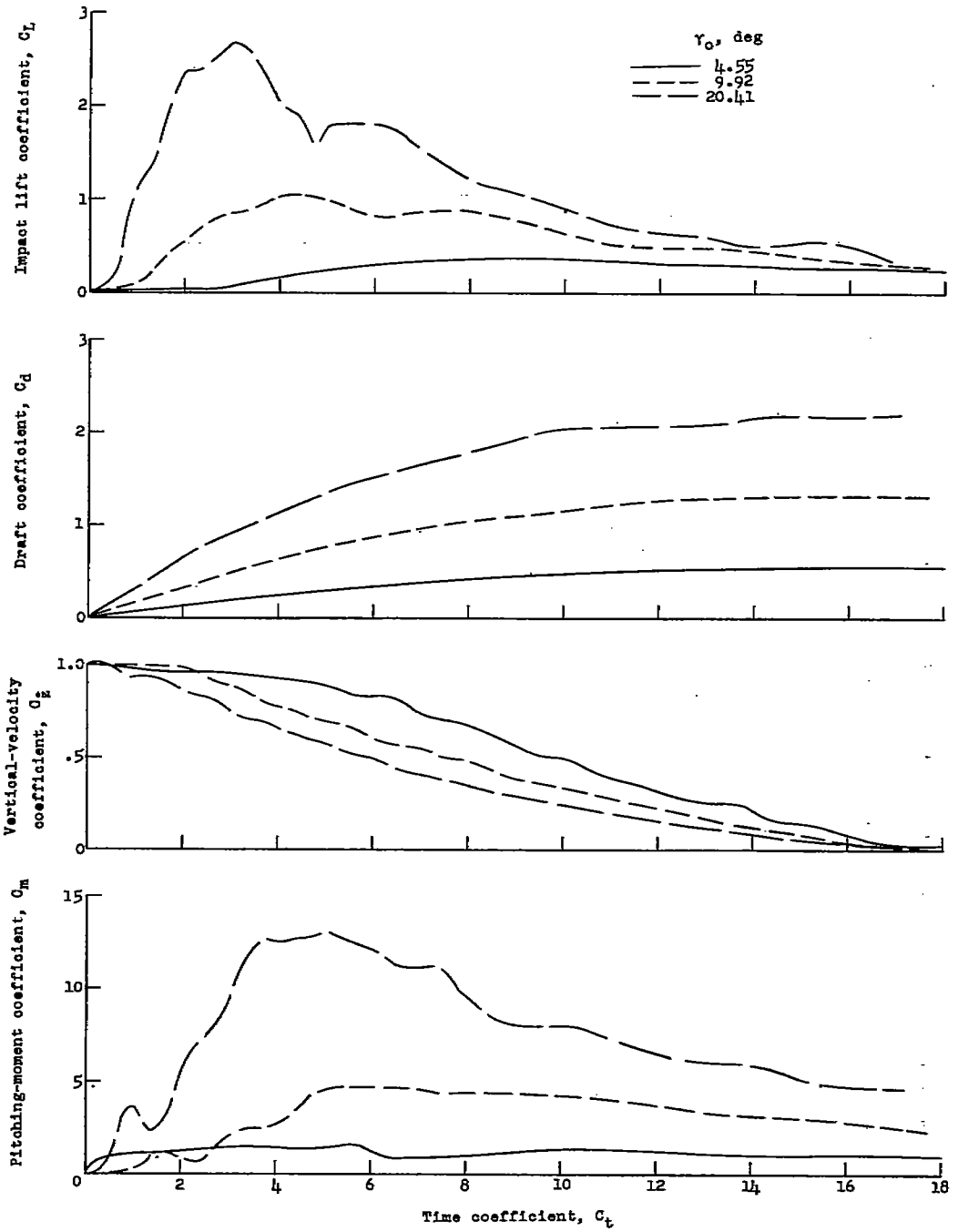

Figure 7.- Variations of the load and motion coefficients with time coefficient for impacts with forward speed. $\tau = 8^o$; $C_\Delta = 36.07$.

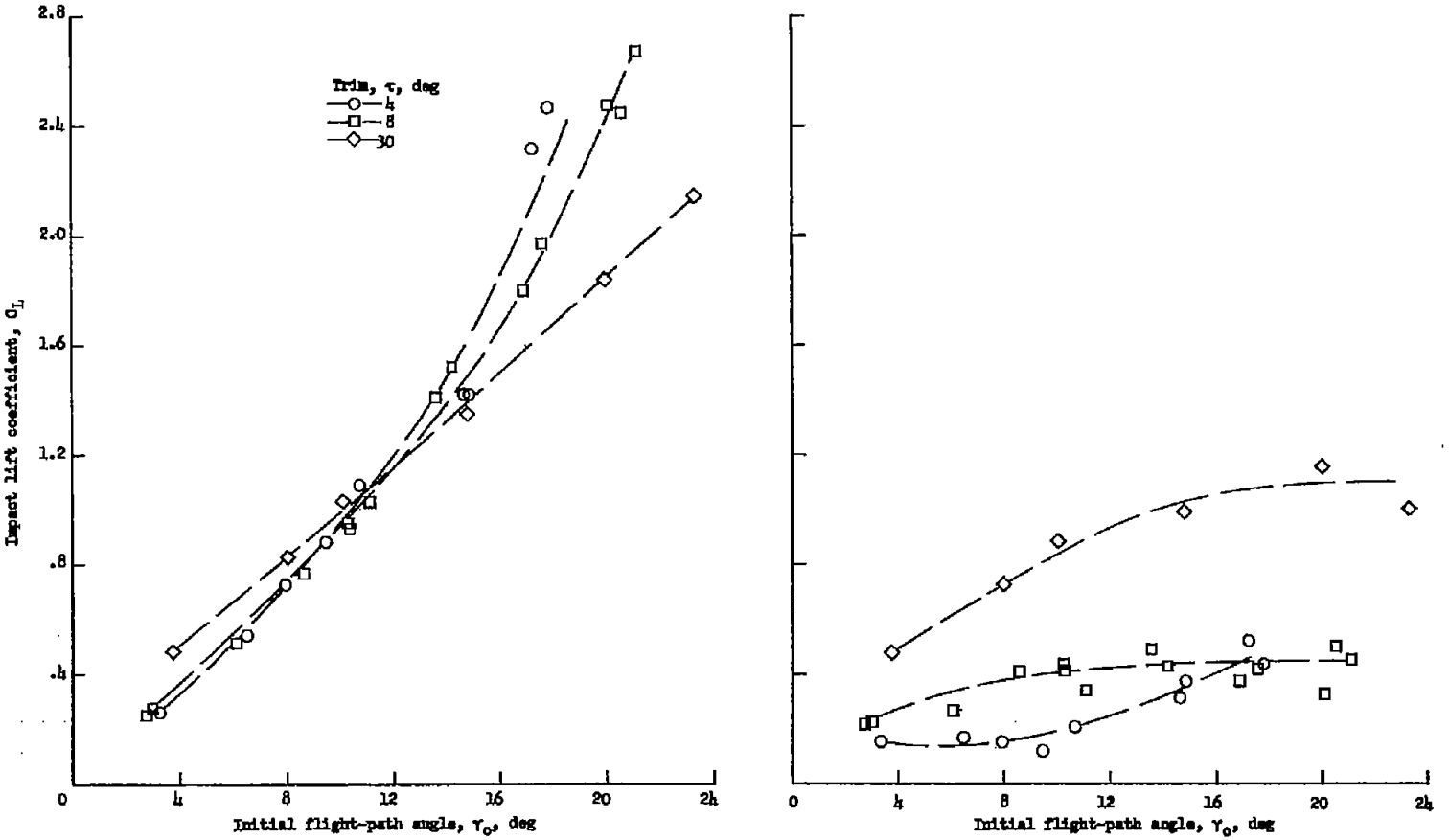

(a) At $n_{i,max}$.

(b) At z_{max}.

Figure 8.- Variations of impact lift coefficient with initial flight-path angle. $C_\Delta = 19.15$.

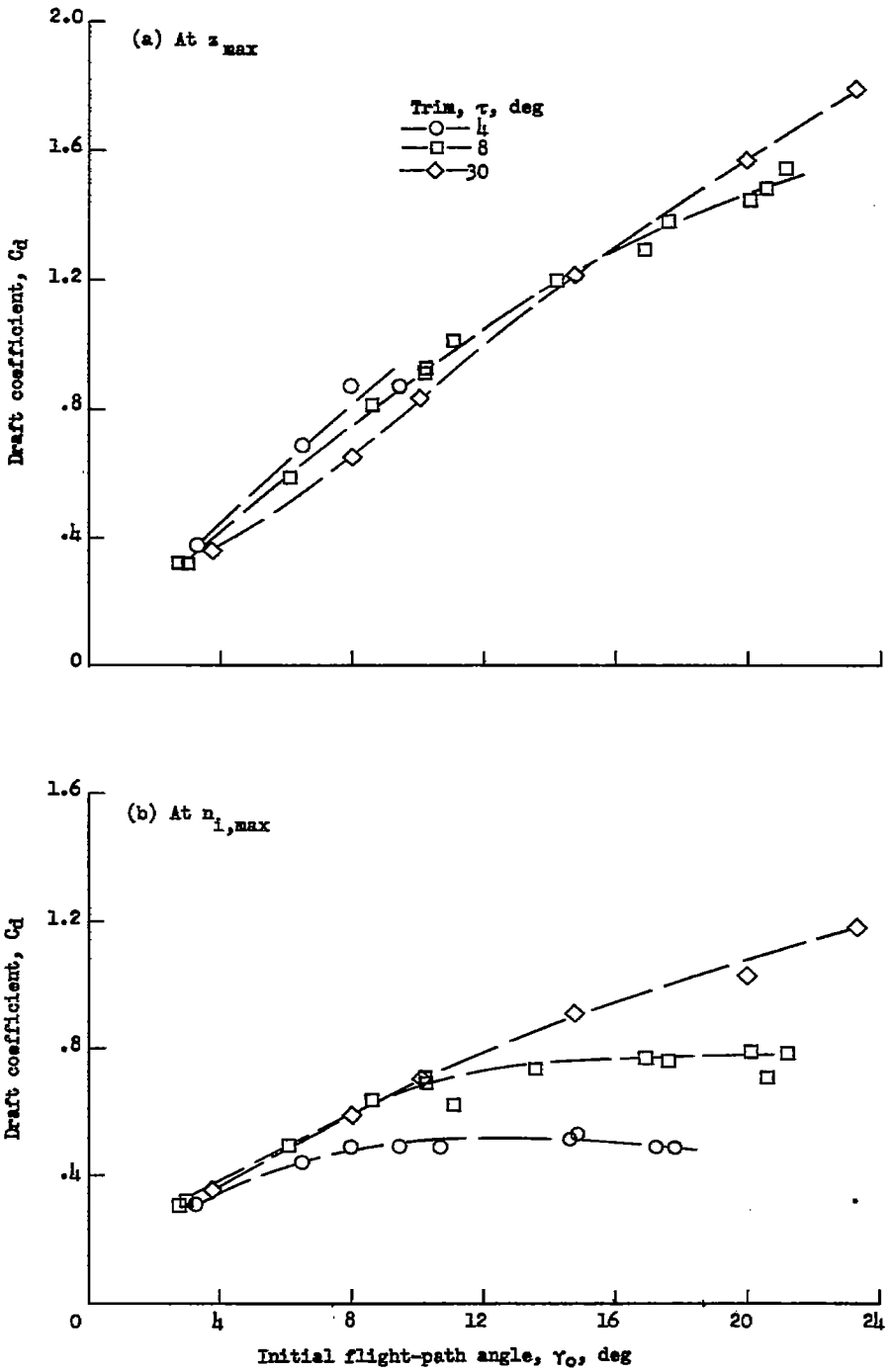

Figure 9.- Variations of draft coefficient with initial flight-path angle. $C_\Delta = 19.15$.

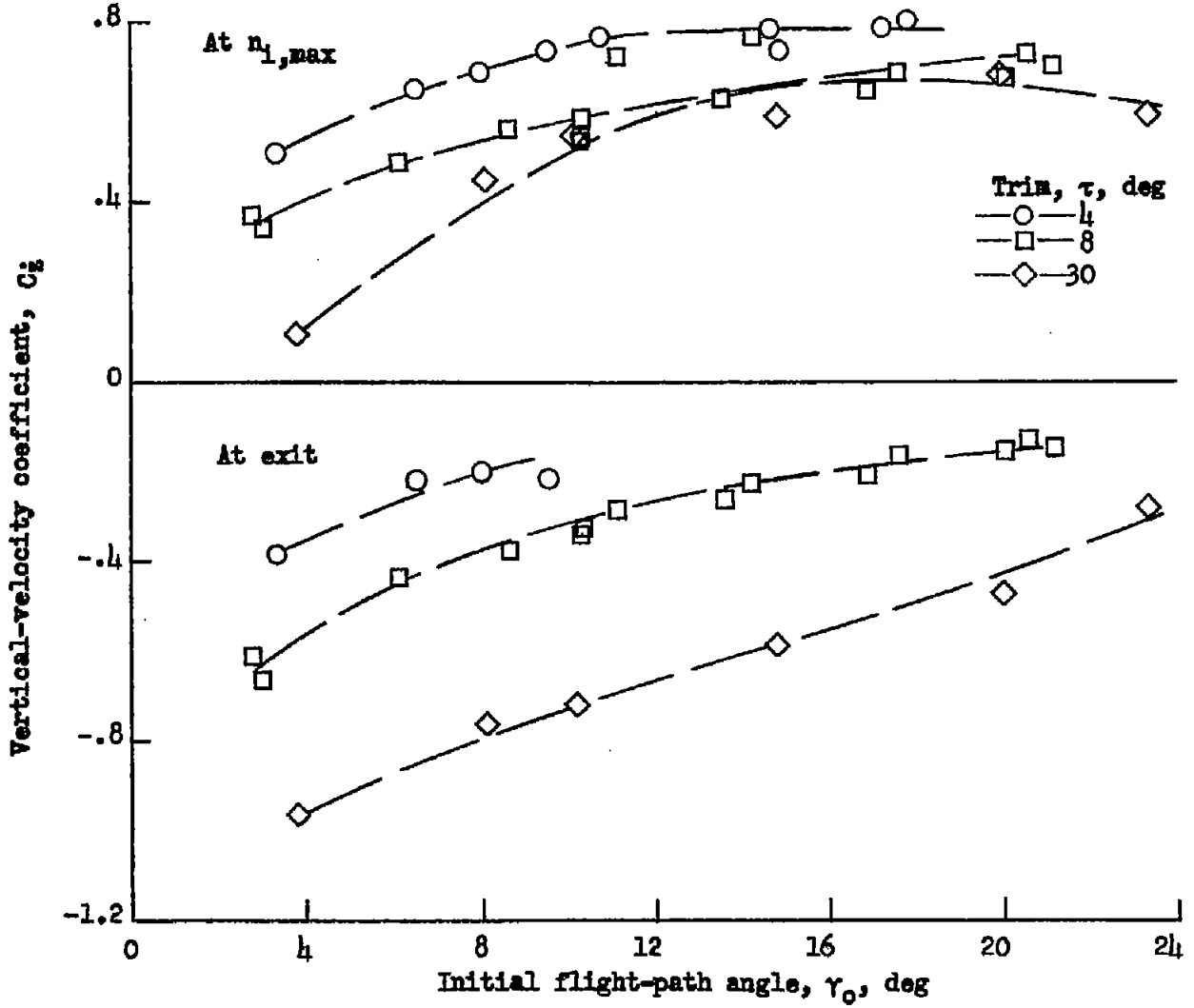

Figure 10.- Variations of vertical-velocity coefficient with initial flight-path angle. $C_{\Delta} = 19.15$.

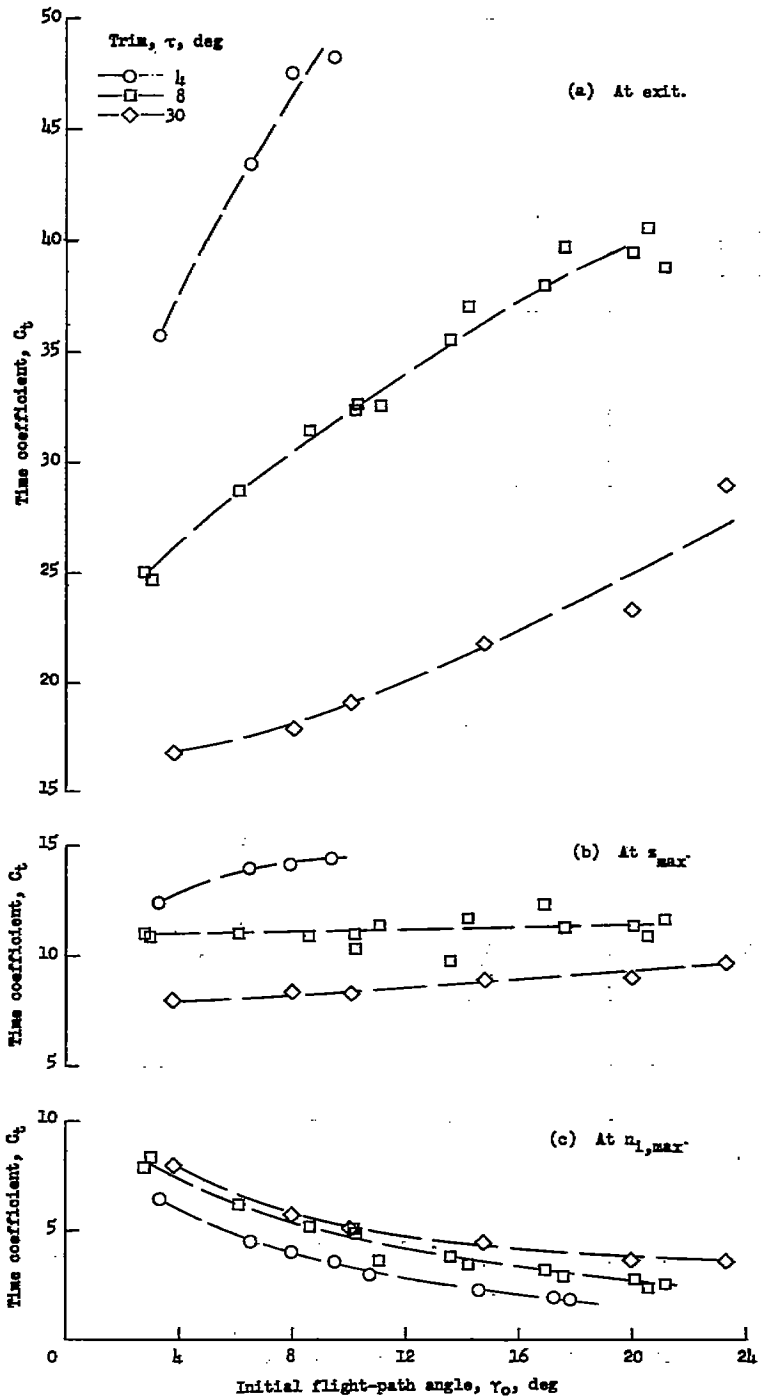

Figure 11.- Variations of time coefficient with initial flight-path angle. $C_\Delta = 19.15$.

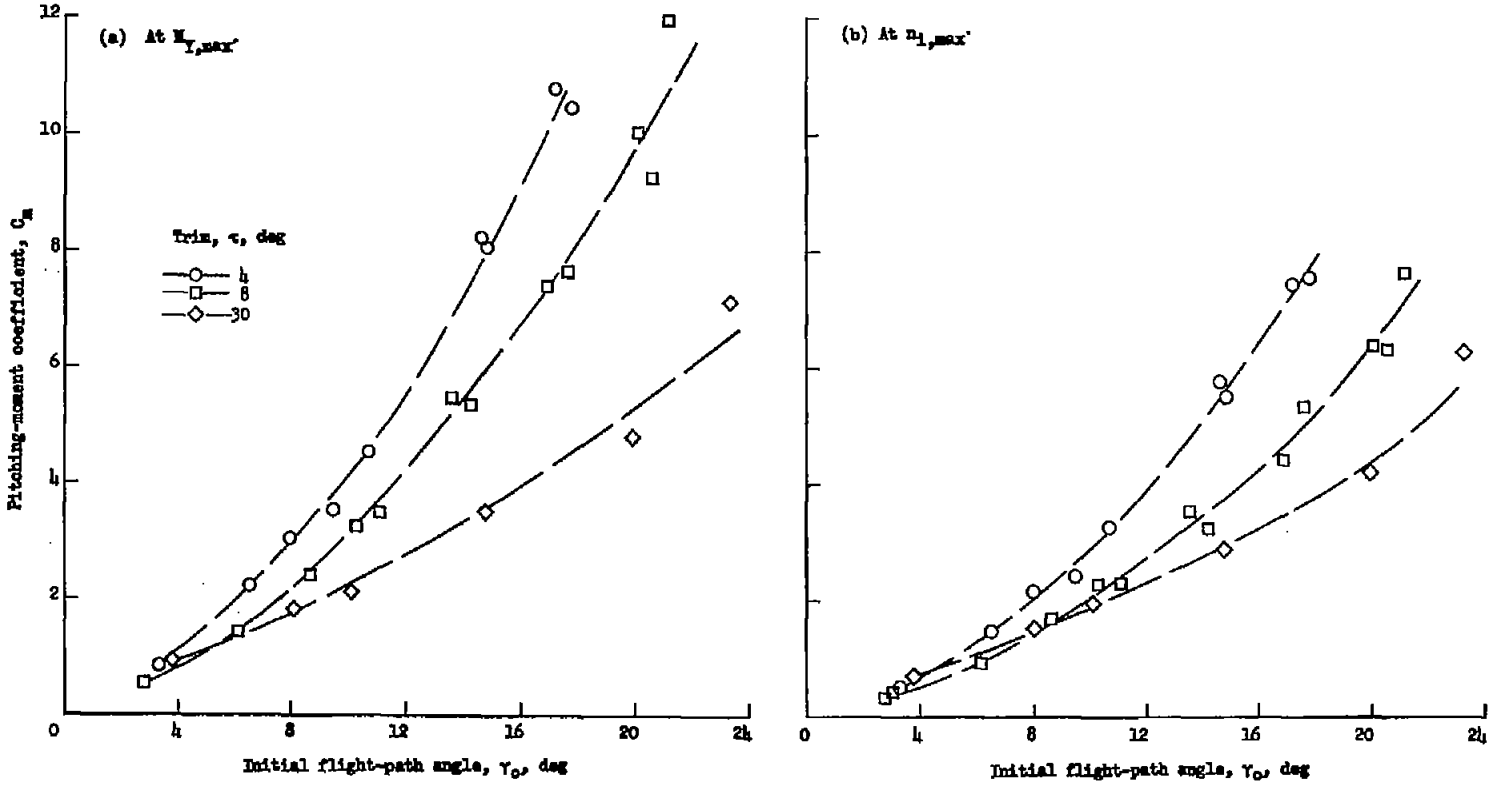

Figure 12.- Variations of pitching-moment coefficient with initial flight-path angle. $C_\Delta = 19.15$.

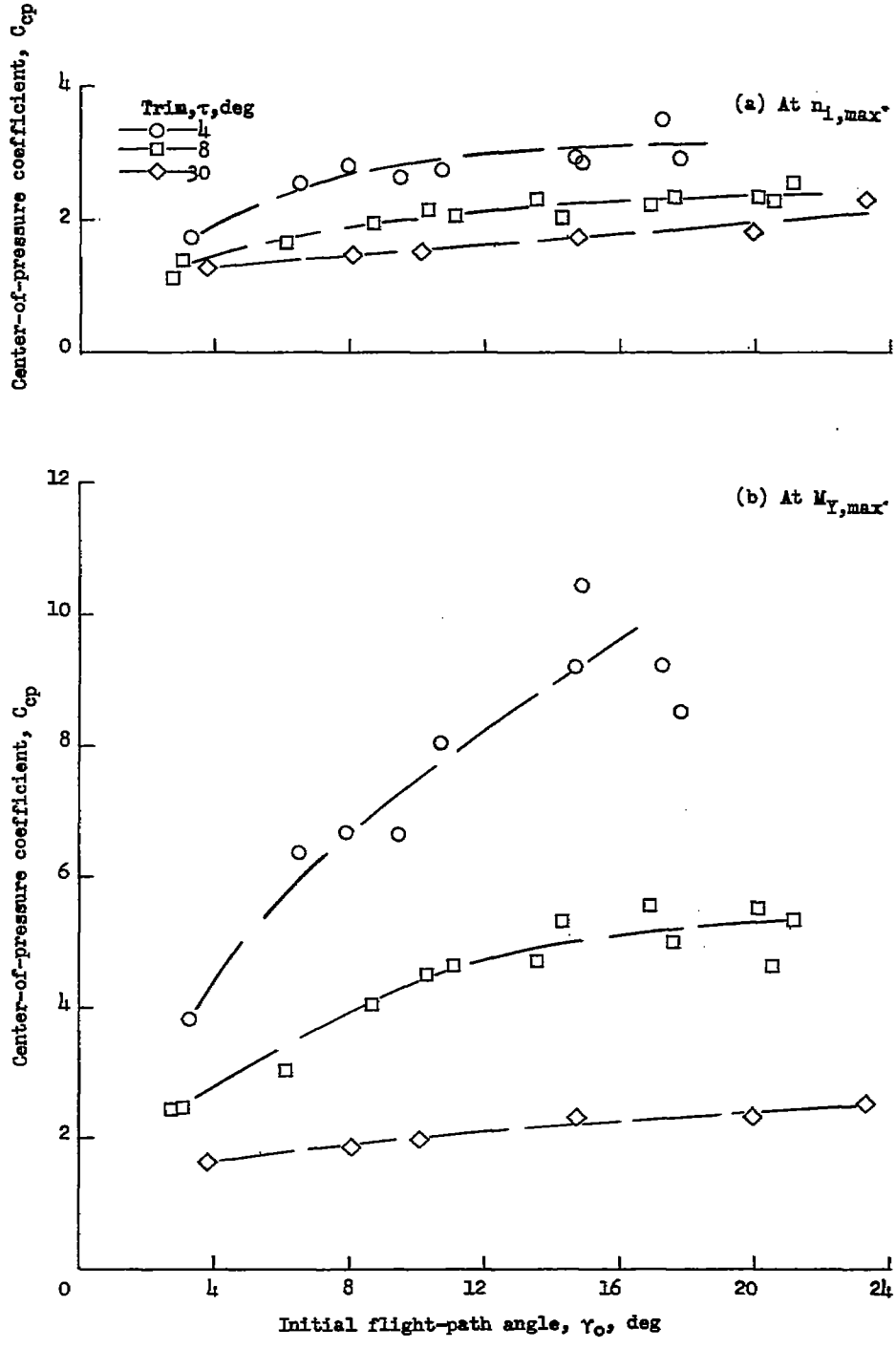

Figure 13.- Variations of center-of-pressure coefficient with initial flight-path angle. $C_{\Delta} = 19.15$.

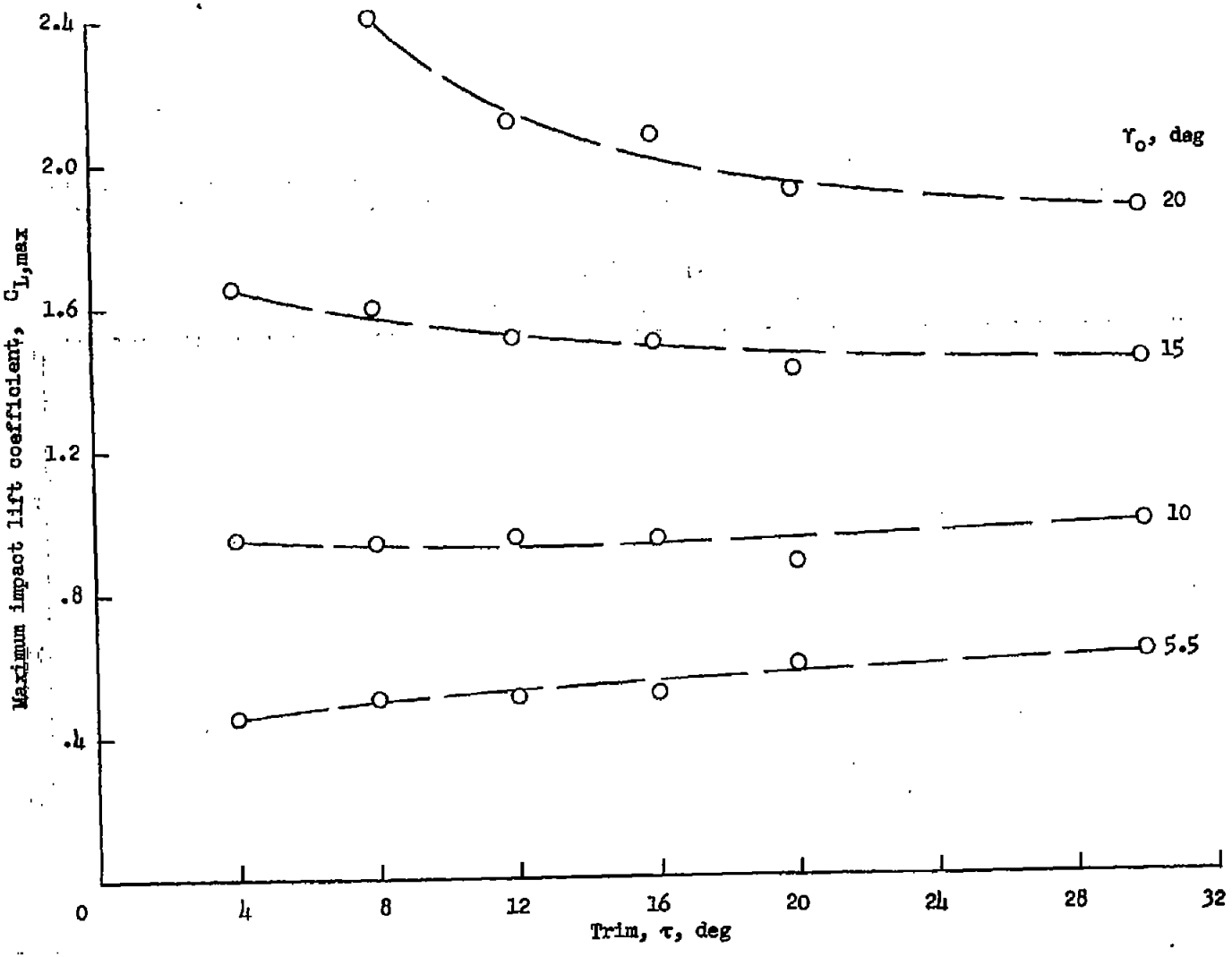

Figure 14.- Variations of faired values of maximum impact lift coefficient with trim angle. $C_\Delta = 19.15$.

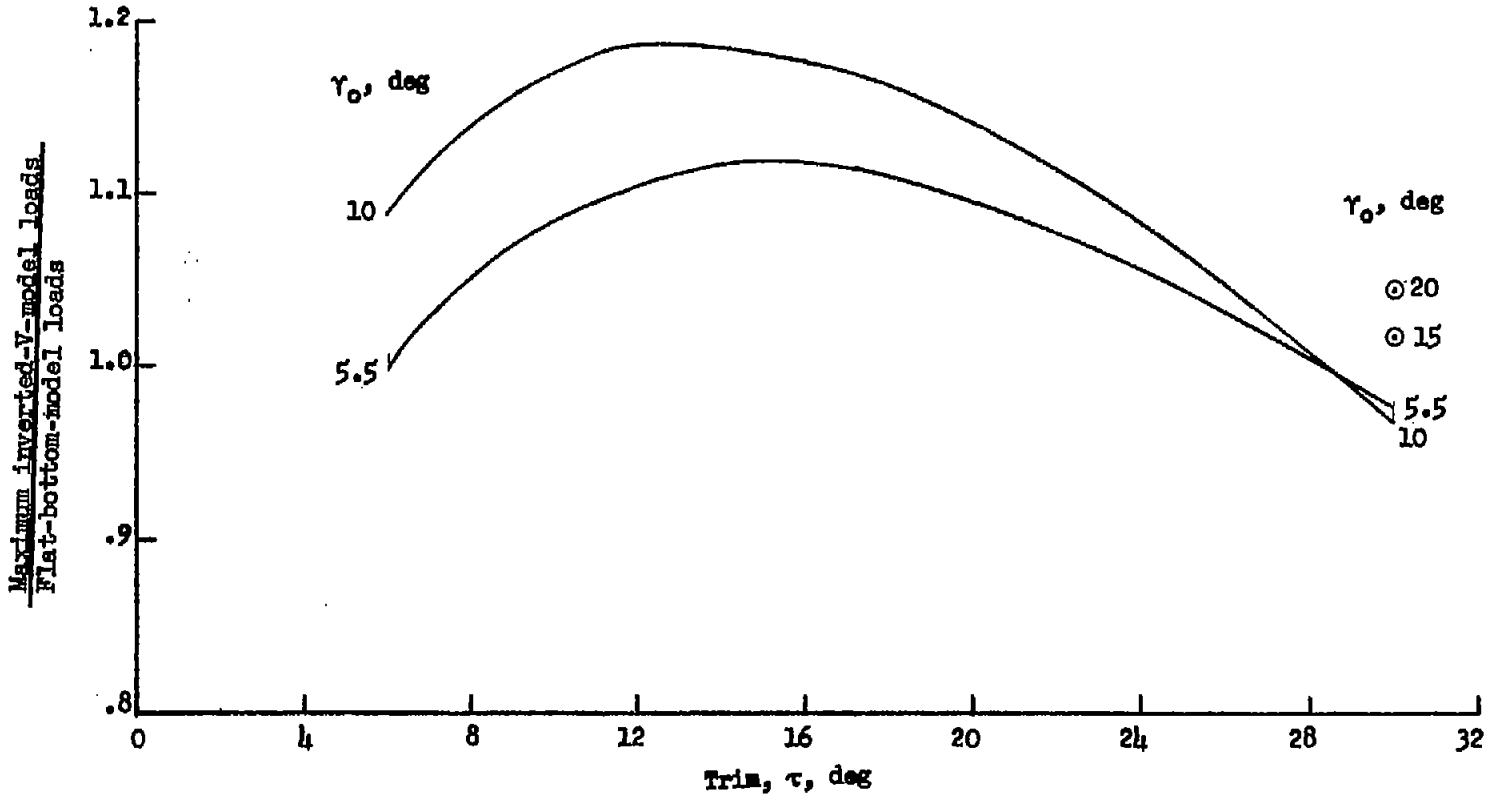

Figure 15.- Variations with trim angle of the ratio of the experimental maximum loads for the inverted-V-bottom model to the experimental maximum loads for the flat-bottom model.

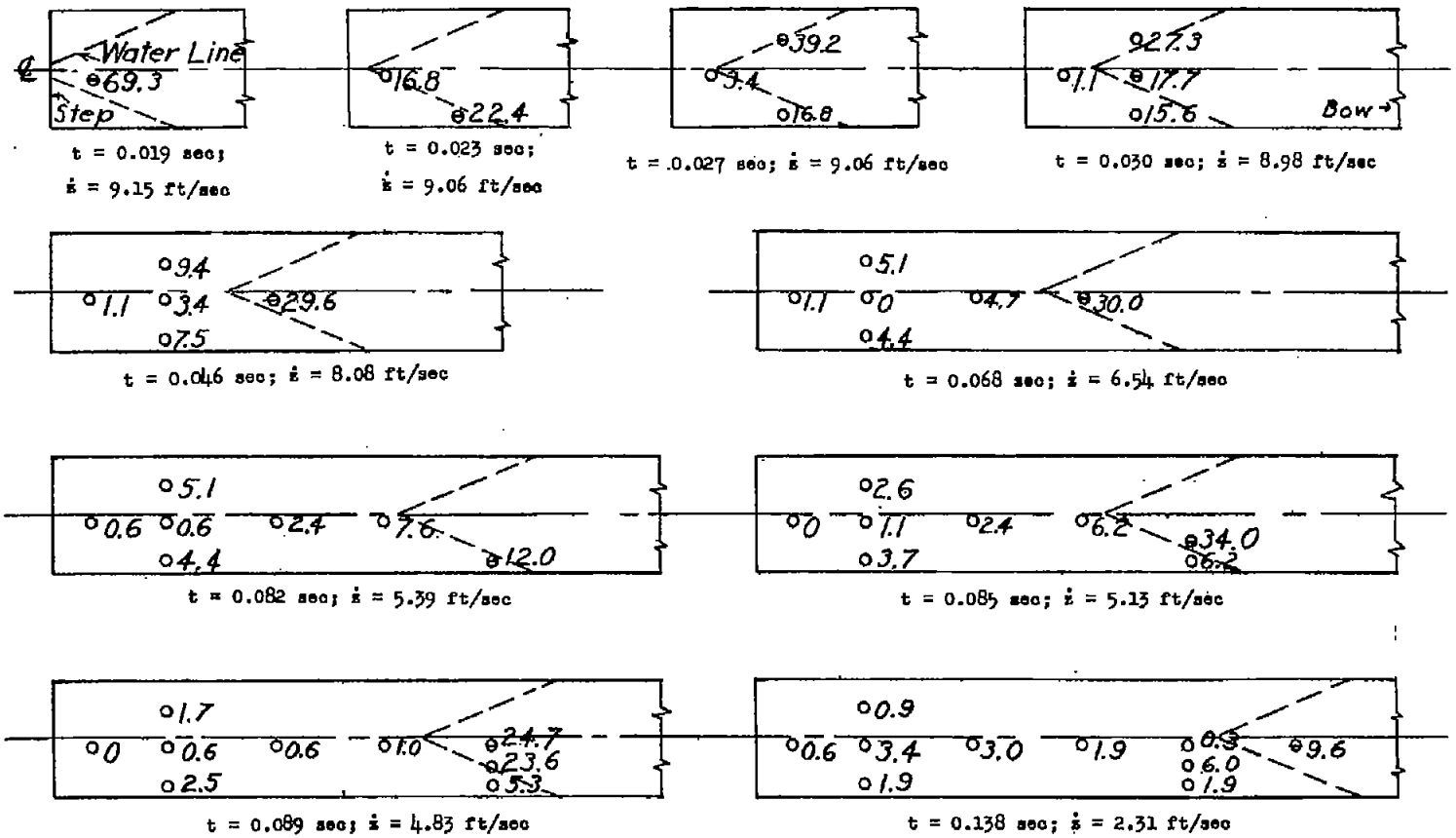

(a) Impact 23: $\gamma_o = 8.64^\circ$; $\dot{x}_o = 61.4$ ft/sec.

Figure 16.- Instantaneous pressure distributions (psi) on inverted-V model having -20° dead-rise angle. $\tau = 8^\circ$; $C_\Delta = 19.15$. (Θ, maximum reading of gage during impact.)

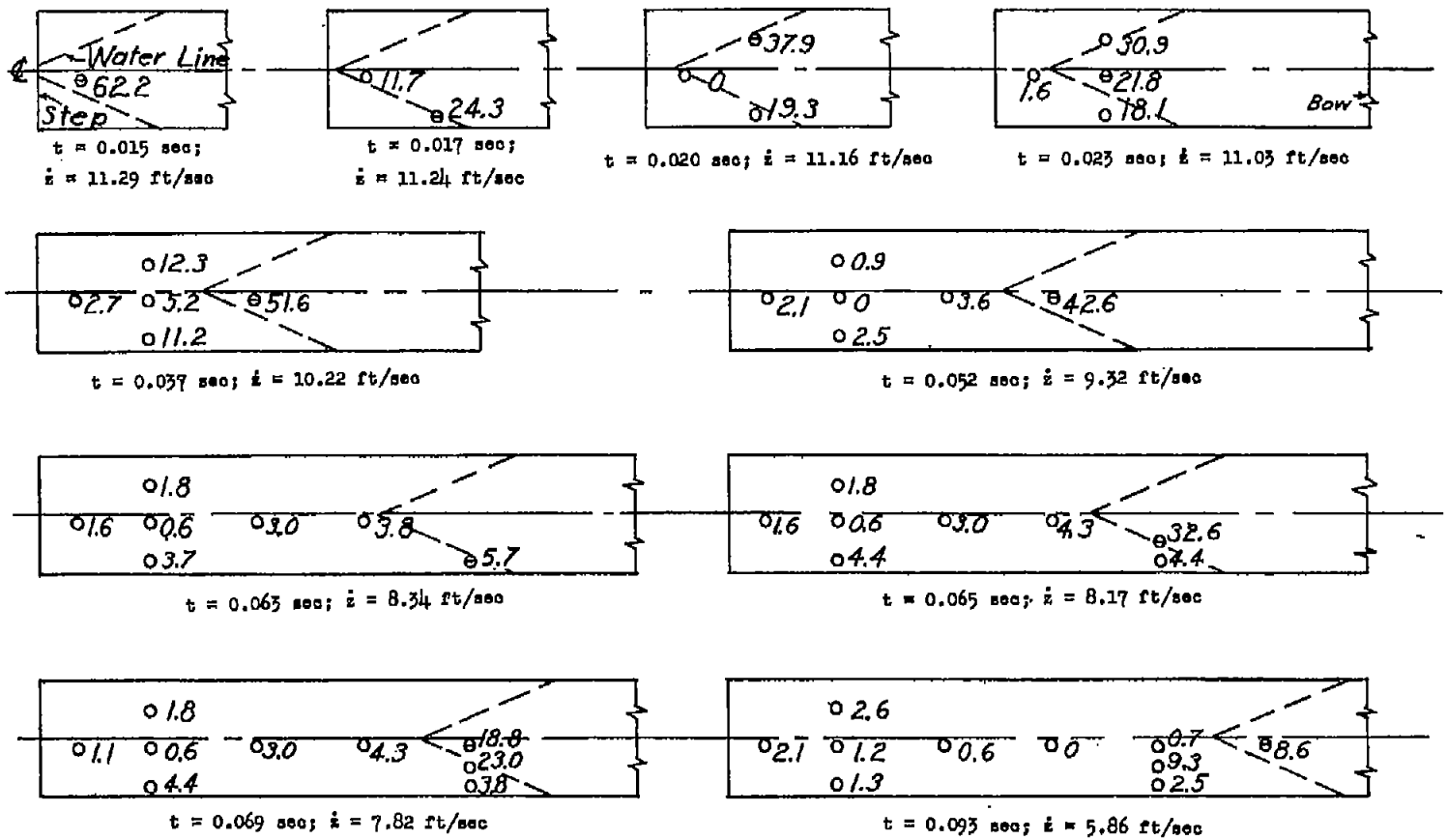

(b) Impact 25: $\gamma_o = 13.58^\circ$; $\dot{x}_o = 46.7$ ft/sec.

Figure 16.- Continued.

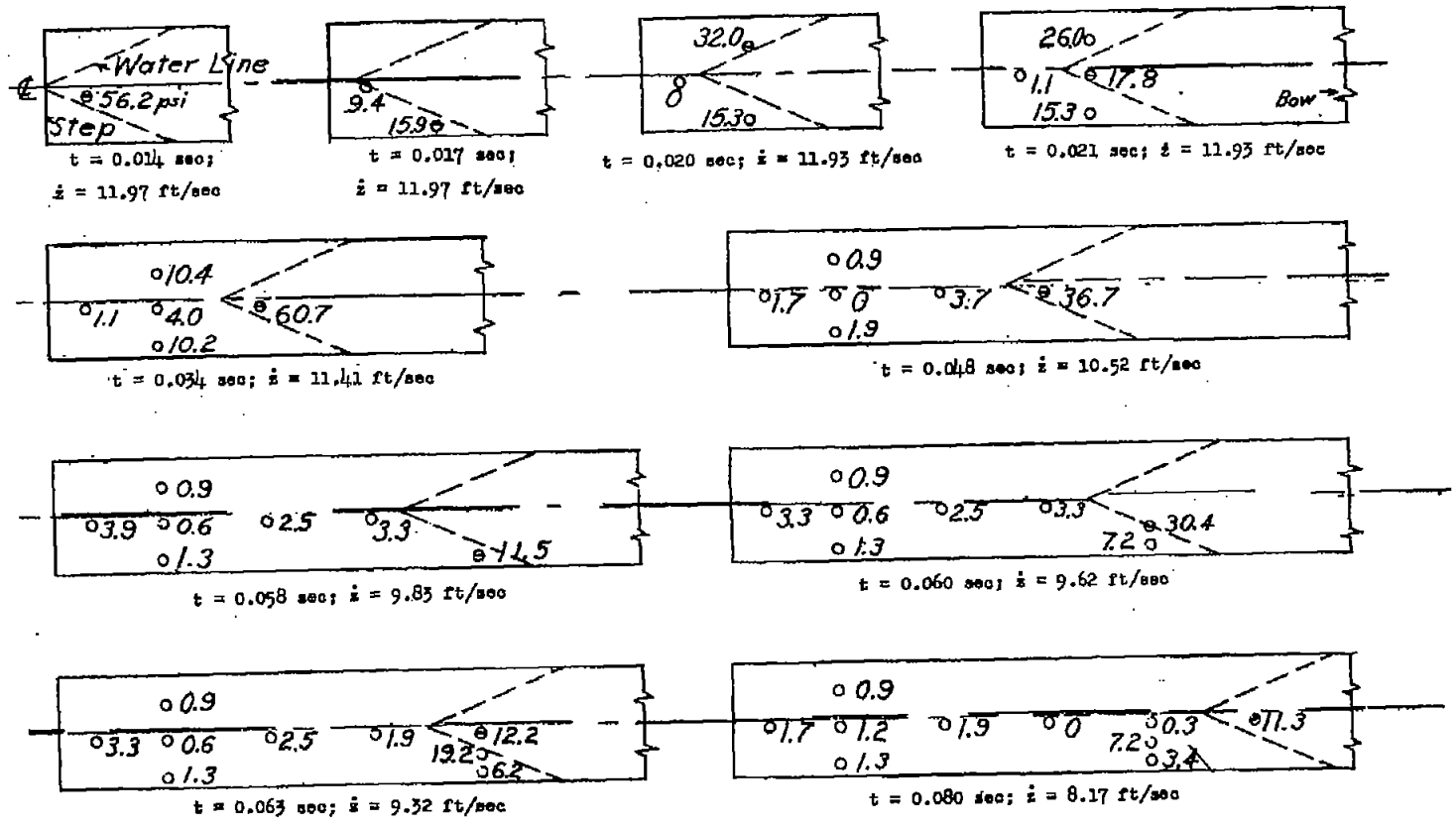

(c) Impact 29: $\gamma_o = 20.06°$; $\dot{x}_o = 32.7$ ft/sec.

Figure 16.- Concluded.

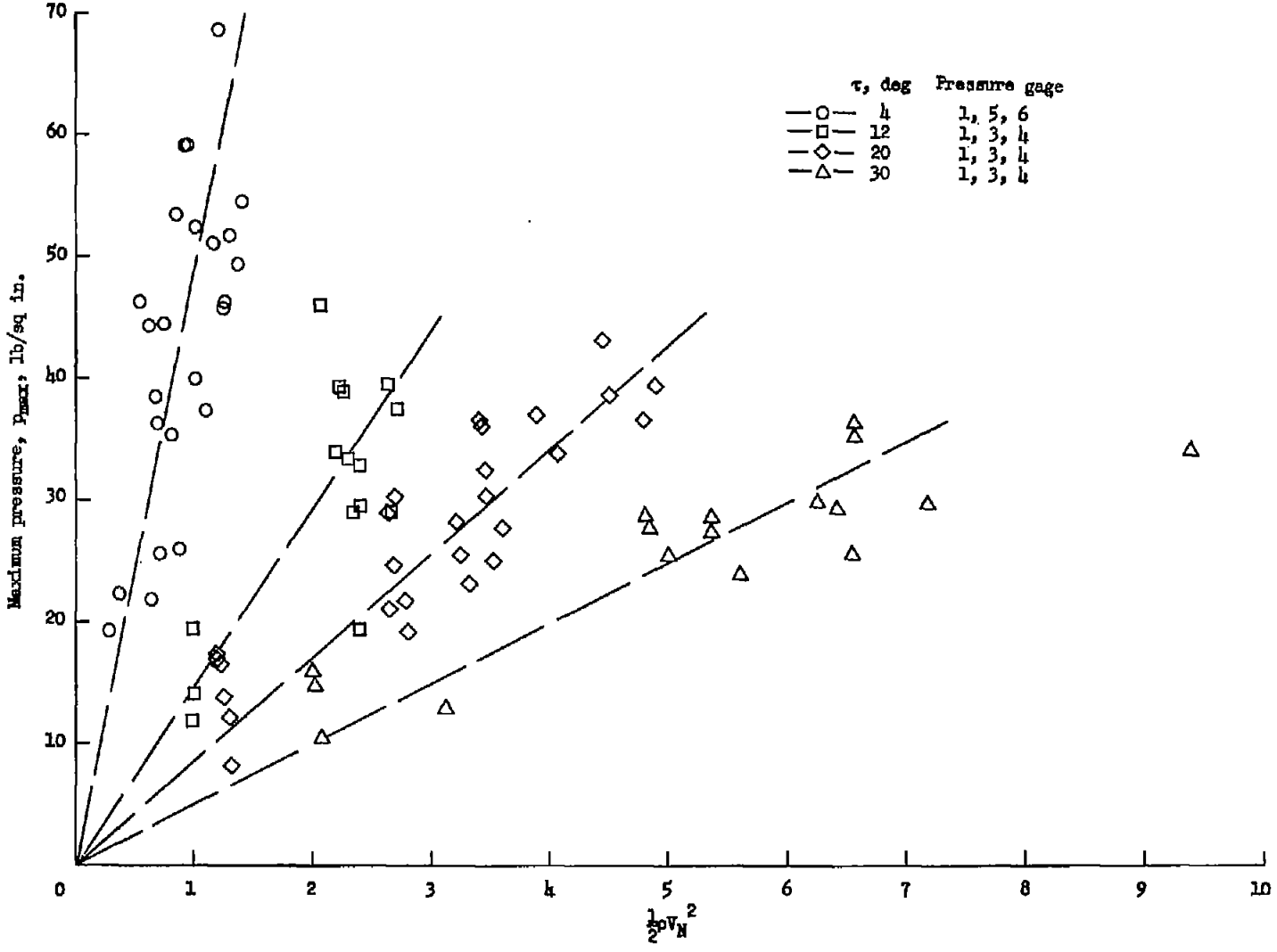

Figure 17.- Variation of maximum pressure with $\frac{1}{2}\rho V_n^2$ for various trims. $C_\Delta = 19.15$.

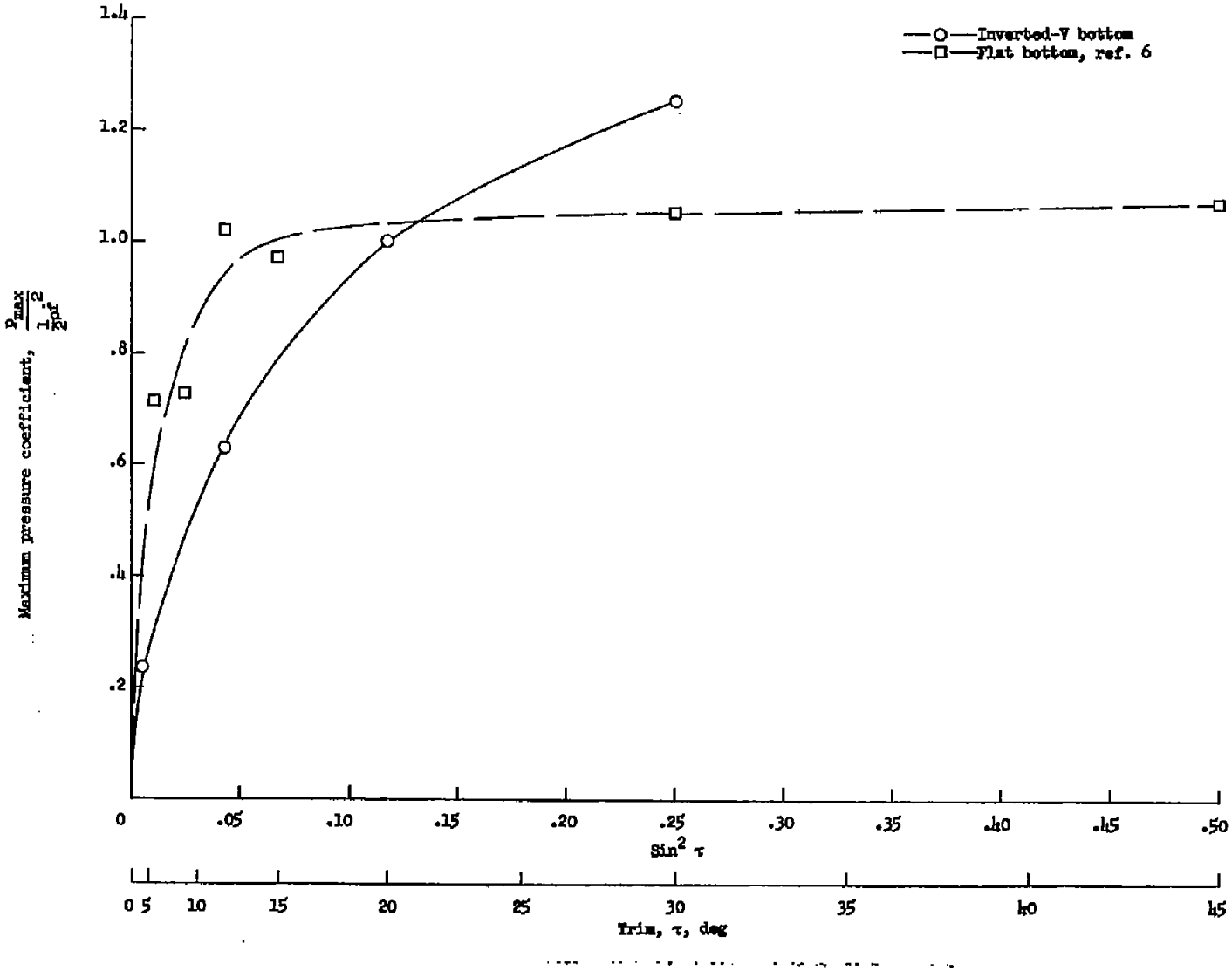

Figure 18.- Variation of maximum pressure coefficient with trim.